

copy 2

Open file - Pittsburgh Univ



IMPLEMENTATION OF A
HIGH SPEED, HEAVY CURRENT,
DC SWITCHING SYSTEM

Prepared for:

UNITED STATES DEPARTMENT OF THE INTERIOR
BUREAU OF MINES

by

Electrical Engineering Department
348 Benedum Hall
University of Pittsburgh
Pittsburgh, Pennsylvania 15261

Type of Report: Final

Contract No.: HO 366013

FEBRUARY, 1978



DISCLAIMER NOTICE

The views and conclusions contained in this document are those of the authors and should not be interpreted as necessarily representing the official policies or recommendations of the Interior Department's Bureau of Mines or of the U.S. Government.

During the course of the research and investigation, a variety of commercial products were utilized and evaluated. Because of the nature of this study and the author's conviction that this report should serve as a design guide, some of the products are listed by manufacturer and by name or catalogue number. Such identification does not, in any fashion, constitute endorsement by USBM of either the product or the manufacturer.

Manufacturers so listed include the following:

- The General Electric Company
- NL Industries
- IBM
- Degussit
- Sauereisen Company
- Synthane-Taylor Company
- Reynolds Industries Incorporated
- Co-Polymer Chemicals, Incorporated
- Rexnord

1. Report No.	2.	3. Recipient's Accession No.	
4. Title and Subtitle Implementation of a High Speed, Heavy Current, DC Switching System		5. Report Date February 1978	
7. Author(s) Howard B. Hamilton, P.I. Elias Strangas, Graduate Student Researcher		6.	
9. Performing Organization Name and Address Electrical Engineering Department 348 Benedum Engineering Hall University of Pittsburgh Pittsburgh, PA 15261		8. Performing Organization Report No.	
12. Sponsoring Organization Name and Address Office of Assistant Director - Mining Bureau of Mines, Department of Interior Washington, D.C. 20241		10. Project/Task/Work Unit No. 5-36941	
15. Supplementary Notes		11. Contract or Grant No. HO 366013	
16. Abstract		13. Type of Report Final	
<p>Laboratory performance of mercury filled current limiting devices (CLD) used for high speed switching of DC circuits (600 volts and below, up to 1000 amperes) using a system involving a parallel connected vacuum switch with CLD and an additional series connected vacuum switch was verified in USBM Contract #HO 357079.</p> <p>This report details analytical work and field experimental tests to predict and control voltage surges associated with the high switching speed associated with the switching system.</p> <p>It also details tests conducted to demonstrate the fault current limiting ability of the CLD.</p> <p>Problems associated with designing a fault current limiting system are discussed.</p>		14.	
17. Originator's Key Words DC Switching Current Limiting Device Low Voltage DC Switching Surges		18. Availability Statement	
19. U.S. Security Classif. of Report None	20. U.S. Security Classif. of Page None	21. No. of Pages 74	22. Price

FOREWARD

This report was prepared by the University of Pittsburgh Electrical Engineering Department, Pittsburgh, Pennsylvania, under USBM Contract Number HO 366013. The contract was initiated under the Coal Mine Health and Safety Program. It was administered under the technical direction of P M & S R C with Mr. Roger L. King acting as the Technical Project Officer. Mrs. Pearl A. Shapert was the contract administrator for the Bureau of Mines.

This report is a summary of the work recently completed as part of this contract during the period January 2, 1976 to January 2, 1978. This report was submitted by the authors on February 28, 1978.

The authors wish to thank Mr. King for his technical advice and suggestions and wish to express appreciation to Mr. King for his assistance in arranging and conducting fields tests at the USDM, Bruceton, Pennsylvania.

EXECUTIVE SUMMARYIMPLEMENTATION OF A HIGH SPEED,
HEAVY CURRENT, DC SWITCHING SYSTEM

Laboratory performance of mercury filled current limiting devices (CLD) was verified in USBM contract #HO 357079. Basically, the switching system which evolved from that research consisted of a parallel connected commercially available vacuum switch and a mercury filled CLD; this combination in series with another vacuum switch, or conventional contactor or circuit breaker.

The CLD consists of two pressurized (3 atmospheres) end reservoirs of mercury connected by a thin filament of mercury. The thin filament of mercury serves as a "vapor chamber." The vapor chamber is a small diameter alumina tube, cast in a castable ceramic and surrounded by an insulating housing which also serves to separate the stainless steel end caps which contain the pressurizing pistons immersed in the end reservoirs.

The normal current path is through the two switches, i.e., the CLD is by-passed. When the switching operation is initiated, the paralleled switch is opened; this commutates, or transfers the current into the CLD. The vapor chamber of the CLD is designed so that the current rapidly (times on the order of 1 millisecond) brings the mercury filament to vaporization temperature. A bubble is formed and the vaporized bubble expands, expelling liquid mercury from the vapor chamber, leaving a vaporized mercury conducting path.

The resistance of the CLD suddenly changes (increases) by a factor of several hundred, thus causing a very marked decrease in the circuit current. This 'change of state' of the CLD is sensed and the second switch, still in series with the circuit current is actuated and completes circuit interruption. The pressurized end reservoirs then reset the CLD by forcing liquid mercury back into the vapor chamber.

With proper design based on circuit parameters, the initial transfer of current from the parallel switch to the CLD can be made arcless. A vacuum switch is suggested for this duty because it is totally isolated from the environment, consists of low mass moving parts and can be quickly actuated. After CLD change of state, the circuit current is at a low level (can be designed such that it is below 15 amperes in 300 and 600 volt DC circuits) and can be interrupted by a vacuum switch, which does have limited current chop capability.

In recognition of the fact that the high rate of change of current involved in the CLD change of state will induce voltage transients in the supply and the disconnected circuit the research described in this report was undertaken to develop techniques for predicting and controlling the voltage surges in actual field tests, as well as to verify the effectiveness of the CLD in switching an actual trolley and in fault current limiting.

A small scale (2000 watt) series motor-shunt generator set was tested using a CLD designed for their rating. Voltage surges were measured when the combination was switched; with and without surge suppression schemes. A comprehensive computer model of the system was developed and also a simplistic approach to predicting the resulting voltage surges was derived. Predictions of surges to be expected with a surge suppression system (combination of electrolytic capacitors, nonlinear resistors and metallic oxide varistors) were made and checked experimentally. Good correspondence between theoretical and experimental results was achieved.

With the confidence in ability to control surges obtained in the lab tests, CLD's were designed for use in a switching system field tested at the USBM above ground trolley system at Bruceton, PA. The tests at Bruceton demonstrated that the switching system performed as designed and that the surges could be controlled.

Also, a CLD designed and installed as a fuse demonstrated the ability of a CLD to limit peak fault current and limit sustained fault current to any desired value.

The report includes a discussion of the problems involved in designing a fault current limiting system and a recommendation for further work in the area.

TABLE OF CONTENTS

	<u>Page</u>
List of Figures	6
List of Tables	9
Nomenclature	10
1.0 <u>INTRODUCTION AND OBJECTIVES</u>	11
1.1 The CLD Switching System	11
2.0 <u>SURGES AND TRANSIENT OVERVOLTAGES</u>	12
DC Switching	17
Primary Load Break Switching	17
3.0 <u>LABORATORY AND MODEL STUDIES</u>	19
3.1 Generator/Switched Motor Tests	20
3.2 Computer Simulation of the System	28
4.0 <u>CLD DESIGN FOR FAULT CURRENT LIMITING</u>	42
4.1 Detection of the Presence of the Fault	44
4.2 Insertion of the CLD	44
4.3 Design of a Fault Limiting CLD	45
5.0 <u>FIELD TESTS</u>	45
5.1 Interruption of the Load Current	46
The Surge Suppressing Scheme	46
The CLD and the Switching Scheme	46
Test Results	48
5.2 The Short Circuit Tests	50
The CLD and the Test Circuit	50
Test Results	52
6.0 <u>CONCLUSIONS AND RECOMMENDATIONS</u>	55
APPENDIX A <u>DESIGN EQUATIONS AND PROCEDURES</u>	58
Design for Switching a Constant Current	60
Design for Switching a Rising DC Short Circuit Current	61
Design for Switching a Rising AC Short Circuit Current	61
APPENDIX B <u>DETAIL DRAWINGS OF CLD (BRUCETON)</u>	64
APPENDIX C <u>NOTES ON CASTING MATERIAL, STRUCTURAL ADHESIVE AND SEALING USED</u>	71
APPENDIX D <u>DECOUPLED CLD/INTERRUPTER SWITCHING CIRCUIT</u>	72
BIBLIOGRAPHY	74

LIST OF FIGURESFigure No.

1	The Characteristics of the Silicon Carbide Varistor Plotted on Log-Log Paper	14
2	Omitted	
3	Simplified Circuit for the Calculation of DC Generator Transient Voltages	15
4	Using a Capacitor to Suppress Overvoltages in a Disconnected Inductance	15
5	Rectified DC Supply System	16
6	Equivalent Circuit for Switching	16
7	Circuit Used for the Pump Back Testing	21
8	Generator Voltage With No Overvoltage Suppressor	22
9	Generator Voltage With 40 μ F Paralleled With the Generator	22
10	Generator Voltage with 100 μ F Parallel With the Generator	22
11	Generator Voltage With 525 μ F Parallel With the Generator (Motor Voltage Clamped With Free Wheeling Diode)	23
12	Motor and Generator Voltage With 900 μ F Paralleled to the Generator	23
13	Motor and Generator Voltage With 1800 μ F Paralleled to the Generator	23
14	Motor and Generator Voltage With 3600 μ F Paralleled to the Generator	24
15	Pump Back System Test #2	24
16	Pump Back System Test #4	24
17	Pump Back System Test #3	25
18	Pump Back System Test #5	25
19	Pump Back System, 212 Volt Operation Diode at Motor	25

Figure No.

20	Pump Back System, 212 Volt Operation No Diode At Motor	26
21	Pump Back System, Typical CLD Voltage and Current Oscillographs	26
22	Block Diagram of the Simulation of the Pump Back System	29
23	The Flow Chart for the Subroutine that Calculates the Steady State Parameters of the Pump Back System . . .	31
24	Generator Voltage, No Suppressors	36
25	Generator Voltage, 40 μ F at the Generator	36
26	Generator Voltage, 100 μ F at the Generator	37
27	Generator Voltage, 525 μ F at the Generator	37
28	Generator Voltage, 900 μ F at the Generator	38
29	Generator Voltage, 1800 μ F at the Generator	38
30	Generator Voltage, 3600 μ F at the Generator	39
31	Generator Voltage of Pump Back System a) Without Varistor b) With Varisotr 212 Volts, 26.5 Amperes	40
32	Generator Voltage of Pump Back System a) Without Varistor b) With Varistor 100 Volts, 21 Amperes	41
33	The Configurations for the Short Circuited Rectifier . . .	41
34	Short Circuited Rectifier Test	43
35	The Electric Circuit in the USBM Facilities at Bruceton	45
36	DC Voltage after Energizing the Transformer 3600 μ F Across the Rectifier	47
37	DC Voltage after Energizing the Transformer No Suppressors Used	47
38	The Electrical Connections of the CLD for the Field Tests	48

Figure No.

39	The Control Circuit	49
40	Field Test Results	50
41	Field Test Results	51
42	Field Test Results	51
43	Test Circuit for the Current Limiting Short Circuit Field Test	52
44	Short Circuit Test #1 0.25 ohm Parallel Resistance	53
45	Short Circuit Test #2 0.25 ohm Parallel Resistance	53
46	Short Circuit Test #4 0.3 ohm Parallel Resistance	54
47	Short Circuit Test #6 0.4 ohm Parallel Resistance	54
A-1	RE vs. σ for Hg and Na at 3 Atmospheres	59
A-2	$\bar{X}, \bar{Y}, \bar{Z}$ vs. Time and Current	63
B	Detail Drawings of CLD Used at Bruceton	64
D-1	Circuit for Decoupling CLD/Interruptor	73

LIST OF TABLES

Table 1	Characteristics of Silicon Carbide Varistors Manufactured by N and L Industries	14
Table 2	Characteristics of Metal Oxide Varistors Manufactured by General Electric	14
Table 3	C required for Various Rectifiers $V_{\max} = 1.6$	19
Table 4	Pump Back System Parameters	20
Table 5	Overvoltages at the Generator of the Pump Back System at 200 Volts, 24 Amperes	27

NOMENCLATURE

A	area of the arc channel, also auxiliary relay
C	capacitor
CB	circuit breaker
CLD	current limiting device
E	electric field
i, I	current
K	constant in the current-time relationship
l	arc channel length
L	inductance
p	total power of arc
PB	push button
q	number of parallel bores
R	radius
r	resistance
r_v	resistance after change of state (vaporized)
r_c	resistance before change of state ("cold")
SW	switch
t	time
V	voltage
V_{arc}	arc voltage
VS	vacuum switch
X_e	leakage reactance
X_m	magnetizing reactance
σ	electrical conductivity
ρ	electrical resistivity

1.0 INTRODUCTION AND OBJECTIVES

Previous USBM sponsored research, USBM Contract Report #HO 357079, entitled "Feasibility Study of the Use of Current Limiting Devices in Interrupting and Sectionalizing of DC Circuits in Mines," presented the theoretical aspects of design and operation of mercury filled current limiting devices (CLD) and the results of laboratory tests on the devices. The feasibility of using such a CLD in conjunction with vacuum switches for switching 300 and 600 volt, DC, in the range up to kiloamperes was established. The speed with which the current limiting effect occurs (millisecond range) was noted and it was recognized that the high rate of change of current would induce transient overvoltages that might be damaging to motors, generators, rectifiers, etc., in the switched circuit.

The report of research and field tests contained herein presents the details of work oriented to the understanding and suppression of the transient overvoltages; field verification of suppression; theoretical design and analysis of CLD useage for fault current limiting and the conclusions derived thereof.

A discussion of DC switching phenomenon, the basic arc physics involved and a derivation of the design equations for the CLD are presented in the USBM Contract #HO 357079 Final Report and are not repeated here. However, use of the design equations and parameters are presented where it is felt appropriate. Reference 1 also presents theoretical data on the CLD.

1.1 The CLD Switching System

The CLD switching system utilizes a mercury filled, change of state (and resistance) device in parallel with a commutating switch and the combination in series with an ultimate circuit interrupter. The purpose of the scheme is to achieve one or more of the following:

- (a) Permit the use of vacuum media enclosed switches (shielding the arcing from the atmosphere);
- (b) Perform a fault current level limiting action;
- (c) Enable a given switch configuration to interrupt a higher current level than would be possible, based on its specific design and conventional usage;
- (d) High speed switching (rapid interruption) to decrease the amount of energy absorbed by the interrupter.

A CLD consisting of one or more (paralleled) thin filaments of mercury (or other liquid metal) exhibits excellent change of state properties for use in this type of system. When the switching cycle is initiated the resistance of the CLD is relatively low, thus permitting easy commutation of the circuit current into the CLD. The mercury vaporizes increasing the resistance by several hundred times and thus driving the current to a very low value, at which time it can be easily interrupted.

The transition from liquid to vapor state, when the CLD operates, is quite rapid, with transition time of the order of 0.5-1.5 milliseconds. The resulting high rate of change of current causes high induced circuit voltages

unless surge suppressing devices are available for absorbing the energy stored in the inductance of the circuit.

Chapter 2 describes the theoretical aspects of the surge suppression problem. In order to evaluate the effectiveness of various proposed schemes, reduced scale tests on small motors and generators were conducted. Chapter 3 details these tests and presents a model of a typical system. Experimental results obtained are compared with theoretical and model predictions. Chapter 4 presents a discussion of the useage of a CLD for limiting the short currents in a DC power supply and the problems associated with this type of application. The field tests and results are presented in Chapter 5. Conclusions and lessons learned are in Chapter 6.

2.0 SURGES AND TRANSIENT OVERVOLTAGES

Changing the electrical conditions of a circuit involves a change and redistribution of the energy stored in inductances and capacitances which will cause transient overvoltages. Specifically, a rapid decrease of current through inductances will generate a higher than normal voltage equal to the inductance times the rate of change of the current. If a fast switching scheme is employed, this rate of change of the current is high as is the resulting overvoltage. If rapid switching schemes are to be developed and utilized, devices and methods have to be found to suppress these overvoltages.

Overvoltages will cause damage both to solid state devices in the circuit and to the electrical insulation of motors or transformers. The most common cause of damage to semiconductor devices occurs when a high reverse voltage is applied to a nonconductive p-n junction. Avalanche currents increase the junction temperature abnormally. This heating releases more carriers which conduct more current in that spot. This action causes melting of the hot spot and the junction is damaged.

The results of overvoltages on insulation are also significant, but usually they are not as obvious as in a damaged diode. The device can continue to operate after a breakdown of its solid insulation, but a localized carbonization will result. Several breakdowns will result in a weakening of the insulation to a point where it will be unable to withstand rated voltage and operating conditions.

In switching heavy current DC circuits, energy stored in the magnetic fields of motors, lines and in the rectifier transformer secondary leakage inductance must be dissipated in either circuit resistance or in arc energy. The energy, during the dissipation period will oscillate between connected or inherent capacitance in the circuit and the inductance present.

Various devices are useful for controlling surges. The most inexpensive and most easily applied is a diode in parallel with an inductive circuit. Diodes are not able to suppress overvoltages, per se, but can be used as a "clamp" by permitting current flow. Hence, the only use of a diode is to suppress a "negative" overvoltage; whereas the diode is not conducting when the normal "positive" voltage is applied. Diodes are, therefore, useful for the protection of motors when the current through

them is interrupted. During normal operation they are reverse biased and nonconducting. These "free wheeling diodes" should have a current rating equal to the rated current of the motors they are protecting and must have a reverse peak voltage (RPV) rating of the maximum positive overvoltage expected during operation of a motor. Free wheeling diodes cannot be used to provide this type of protection for a generator, as source.

Another device specifically designed for surge protection is the "gas breakdown device." These devices depend on the formation of an arc between electrodes. The arc impedance is low, initially, and increases with time, since the arc is deflected along a gradual and continuously increasing spacing between the electrodes. This arc can be reignited after it is extinguished, if the total energy stored in the inductances has not been dissipated. Such a device can dissipate energy on the order of thousands of joules. It can limit the overvoltage to a value not more than two per unit and is excellent for the protection of solid state devices.^{(2)*}

In addition to the high cost of this device, its main drawbacks are that it is often capable of maintaining the arc with the steady state voltage level and often it is not feasible for use at lower voltage levels.

Nonlinear resistors, fabricated from silicon carbide milled and mixed with a ceramic binder have been used for surge suppression. They are available in disk, rod or washer form. Their electrical characteristics are described by the equation⁽³⁾:

$$I = \left(\frac{E}{c}\right)^n = k E^n \quad (1)$$

where:

- I = instantaneous current
- E = instantaneous applied voltage
- c, k = constants
- n = an exponent

The constants c and k depend upon the resistivity, the geometry, and the exponent of the unit under consideration. The exponent, n, depends upon various factors and is usually higher than 2 while that of a linear resistor is 1. Equation (1) can be plotted on logarithmic paper and the characteristic of the resistor then becomes that of a straight line; its suppressing ability determined by its gradient. (See Figure 1) The thermal rating is relatively high. It can dissipate 25W per square inch of surface in still air at room temperature. It can also absorb 2000 joules per cubic inch for a short time impulse. The main problem associated with it is the rather "soft" characteristic, which, for good suppression properties would require the normal operating point to be high on the curve, resulting in a high current for "stand by" operation.

Table 1 shows the characteristics of some silicon carbide varistors manufactured by N & L Industries.⁽⁴⁾ It should be noted that the exponent n varies from 4.5 to 5.3 and that the discharge capacity in joules is quite high.

* Numbers superior to the printed text line denote references detailed in the Bibliography of this report.

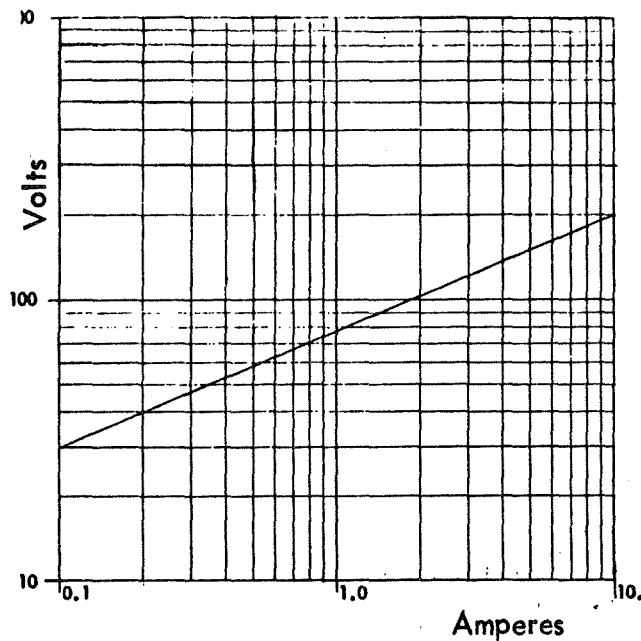


Figure 1. The Characteristics of a Silicon Carbide Varistor Plotted on Log-Log Paper.

TABLE 1

Characteristics of Silicon Carbide Varistors Manufactured by N&L Industries

<u>Operating DC Voltage</u>	<u>Discharge Capacity in Joules</u>	<u>Exponent n</u>	<u>Serial No.</u>
100	3400	4.51	9RV3A11
200	22500	4.52	68W60200
275	22500	5.12	69W60100
300	275	4.77	71D10000
300	51000	5.30	9RV3A14

The latest breed of ceramic type suppressors are commercially known as Metallic Oxide Varistors (MOV) and they possess strongly nonlinear characteristics. They consist mainly of zinc oxide and bismuth oxide that form a polycrystalline semiconductor composed of crystals and grain boundaries. Table 2 shows the main characteristics of some units manufactured by General Electric. As observed, their main advantage is the very high value of exponent n , whereas their disadvantage lies in their relatively low discharge capacity.

TABLE 2

Characteristics of Metal Oxide Varistors Manufactured by General Electric

<u>Operating DC Voltage</u>	<u>Discharge Capacity in Joules</u>	<u>Exponent n</u>	<u>Serial No.</u>
215	20	28	V150PA206
330	40	27	V250PA406
170	20	28	V130PA206

The simplest of surge suppression schemes is the basic capacitor. Essentially, the energy stored in the inductance and capacitance will be transferred back and forth between the two devices. An oscillatory voltage will occur, with a peak value depending on the energy stored and on the value of the capacitance used. The problems associated with this scheme are the high inrush currents, resulting when it is energized and the long duration of the oscillation, since the energy stored in the inductance is dissipated in the usually small resistance of the circuit (an underdamped system).

In the most simple configurations two arrangements of L and C are possible -- in series connected to the source (with load switched) as shown in Figure 3 or as a disconnected parallel connected unit, as shown in Figure 4.

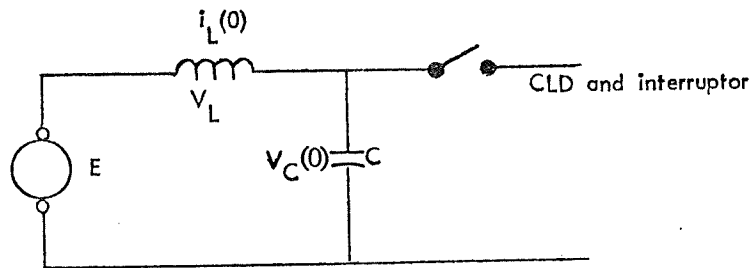


Figure 3. Simplified Circuit for the Calculation of DC Generator Transient Voltages.

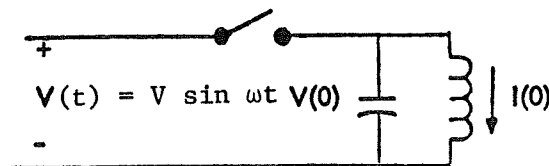


Figure 4. Using a Capacitor to Suppress Overvoltages in a Disconnected Inductance.

The circuit shown in Figure 3 depicts a DC generator supplying a load with current $I(0)$ when the load is switched. Capacitor C provides surge protection and is charged to voltage $V_C(0)$ prior to load switching. Neglecting the resistance of the supply circuit, $V_C(0) = E$ and it is easily shown that the voltage across the capacitor is given by:

$$V_C(t) = V_C(0) + I(0)\sqrt{\frac{L}{C}} \sin \frac{1}{\sqrt{LC}} t \quad (2)$$

yielding, for $V_C(0) = E$, a maximum value of

$$V_{C \max} = E + I(0)\sqrt{\frac{L}{C}} \quad (3)$$

The circuit of Figure 4 depicts an AC energized situation and may be representative of disconnection of an unloaded transformer for example. The worst case situation here is where $I(0)$ is a maximum, $V(0) = 0$ and, from equating energy stored in L to the same quantity transferred to C;

$$V_c \max = I(0) \sqrt{\frac{L}{C}} \quad (4)$$

Figure 5 depicts the situation where in a 3 phase, full wave rectifier is supplied from a transformer with primary switching capability as well as load side DC switching.

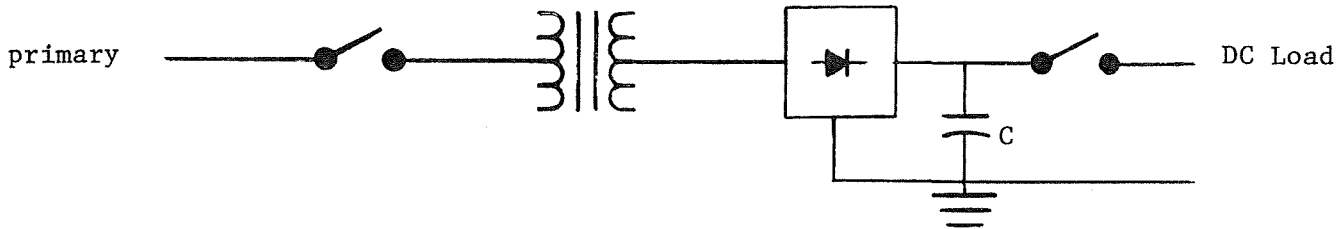


Figure 5. Rectified DC Supply System.

Capacitance located as shown in Figure 5 can be used to suppress surges, or transient overvoltages for either supply or load side switching. The presence of the rectifier between the DC terminals of the capacitor and the 3 phase supply insures that the phases with the highest voltage between them are always connected across the capacitor. An exact analysis of the 3 phase circuit with successive phase interruption is a complex problem, and if transformer saturation is included, must be handled by complex computer algorithms or by a transient Network Analyzer. In the interest of a simple approach, easily applied, the analysis presented below was developed. The results obtained experimentally bear out the validity of the approach, with reasonable accuracy.

Figure 6 depicts the energy storage elements involved in the switching operations

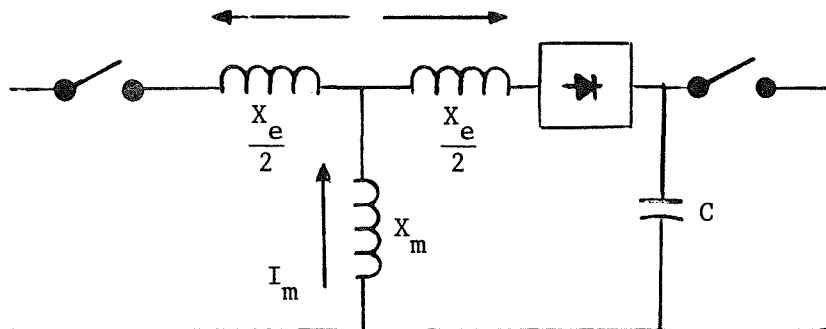


Figure 6. Equivalent Circuit for Switching.

- Define: X_e = total per unit leakage reactance
 X_m = per unit mutual reactance
 I_m = per unit magnetizing (no load) current
 Z_b = base impedance
 I_L = per unit load current
 ω = $2\pi f$, where f = frequency in hertz
 I_b = base current

KV_b = base voltage

MVA_b = base megavolt amperes.

DC Switching

When switching on the DC side, the transformer core remains magnetized and only the energy stored in the leakage inductance of the secondary winding need be absorbed by the capacitor. That stored energy, W_s is:

$$W_s = \frac{1}{2} \left(\frac{X_e}{2\omega} Z_b \right) (\sqrt{2} I_L I_b)^2 \text{ joules} \quad (6)$$

Noting that:

$$Z_b = \frac{KV_b^2}{MVA_b} \quad \text{and} \quad I_b = \frac{(MVA_b) 1000}{\sqrt{3} KV_b} \quad (7)$$

Equation (6) becomes; for three phase, i.e., total secondary stored energy (max current in one phase, one half of max in the other two phases)

$$W_s = \frac{(X_e) (MVA_b) (I_L)^2 10^6}{4\omega} \text{ joules} \quad (8)$$

The capacitor is charged to a voltage of $\sqrt{2}$ times the transformer secondary rms line-line voltage. Since the DC voltage, E_{dc} is 1.35 times the rms line-line voltage, $V_c(0)$, the capacitor voltage, E_{dc} when switched is found as follows:

$$\begin{aligned} E_{dc} &= 1.35 V_{rms} \\ V_c(0) &= \sqrt{2} V_{rms} \\ V_c(0) &= \frac{\sqrt{2}}{1.35} E_{dc} = 1.05 E_{dc} \end{aligned} \quad (9)$$

The energy W_s , from (8) must be added to the energy stored at the time of switching. Thus

$$\frac{1}{2} CV_m^2 - \frac{1}{2} CV_c^2(0) = W_s \quad (10)$$

or

$$V_m = \sqrt{1.1 E_{dc}^2 + \frac{1}{2C} \left\{ \frac{(X_e) (MVA_b) (I_L)^2 10^6}{\omega} \right\}} \quad (11)$$

where, V_m = maximum voltage across the capacitor and X_e , I_L are given in per unit on the transformer MVA_b base.

Primary Load Break Switching

Neglecting the arcing energy absorption associated with primary load break switching, the capacitor must absorb all stored energy in the transformers, W_t .

Total energy stored in the leakage inductance is, from (8)

$$W_s + W_p = \frac{2(X_e)(MVA_b)(10^6)(I_L)^2}{4\omega} \quad (12)$$

Similarly, energy stored in the magnetizing inductance is:

$$W_m = \frac{(X_m)(MVA_b)(10^6)(I_m)^2}{4\omega} \quad (13)$$

However, I_m and I_L are nearly in quadrature. It can be shown that extremes exist when I_m is a maximum and I_L is zero and vice versa. To determine the true maximum, the ratio of W_m to $W_p + W_s$ is examined

$$\frac{W_m}{W_p + W_s} = \frac{X_m I_m^2}{X_e I_L^2} \approx \frac{I_m}{X_e I_L} \quad (14)$$

Since, $I_m \approx 0.03 I_L$ and $X_e \approx 0.08$

$$W_m \approx \frac{3}{8}(W_p + W_s) \quad (15)$$

Therefore, consider the worst case of stored energy oscillation into the capacitor as the time when I_L is a maximum, yielding (as with equation (10) and (11) but noting that the energy stored in both windings will enter the capacitor,

$$V_m = \sqrt{1.1 E_{dc}^2 + \frac{1}{C} \left\{ \frac{(X_e)(MVA_b)(I_L^2)(10^6)}{\omega} \right\}} \quad (16)$$

It should be noted that surge suppression capacitor location as analyzed above does not provide surge protection for the rectifier unit for surges that travel in from the primary supply (lightning and externally generated surges).

In order to obtain a visualization of the size of capacitors required in typical switched rectifier installations, several 60 Hertz sizes were evaluated. In the evaluation, it was assumed that V_m would be limited to 1.6 per unit E_{dc} and that transformer leakage reactance was 0.08 per unit. The values calculated are presented in Table 3.

It might appear that these are large values of capacitance required. However, it should be noted that inexpensive, dry, electrolytic capacitors rated 500 volts, 1800 microfarads are available. Series/parallel combinations to yield 1.6 per unit overvoltage limitation can be easily connected.

In order to provide a safety bleed resistance in parallel with the capacitors and to provide an added margin of conservatism in the overvoltage calculations as well as to absorb and dissipate the stored energy, it is recommended that varistor assemblies be paralleled with the capacitors.

TABLE 3

C Required for Various Rectifiers; $V_{\max} = 1.6$ p.u.

<u>Rectifier</u>	<u>I_L, per unit</u>	<u>C Required, Microfarads</u>
$E_{dc} = 300$ Kva = 300	1.0	698
	2.0	2795
	4.0	11177
$E_{dc} = 600$ Kva = 300	1.0	175
	2.0	699
	4.0	2794
$E_{dc} = 300$ Kva = 1000	1.0	2329
	2.0	9315
	4.0	37258
$E_{dc} = 600$ Kva = 1000	1.0	582
	2.0	2328
	4.0	9315

The data sheet in NL Varistors, of the 9RV3 series is a part of this report. As an example of varistor selection, consider the use of the 9RV3A14 unit rated 300 volts continuous with a continuous power loss of 3 watts, corresponding to a resistance at 300 volts of 30,000 ohms. As a bleed resistor, this yields a time constant of 54 seconds with 1800 microfarad of capacitance. The 9RV3A15 is suitable for 600 volt service.

Summarizing, dry electrolytic capacitors, connected in series/parallel and paralleled with a varistor energy absorber and bleeder appear to offer an inexpensive, effective means of suppressing surges induced by high speed switching of rectifier or generator DC power supplies of the size currently used in mining operations. A free wheeling diode, switched in shunt with the motor type loads will clamp "negative" type overvoltages associated with motor switching.

To verify these conclusions, laboratory tests on reduced scale systems were conducted and are detailed in the following chapter.

3.0 LABORATORY AND MODEL STUDIES

In the first tests the CLD was used to interrupt the current flowing from a shunt connected DC generator into a series motor. The objective of these tests was to obtain data about the operation of the CLD in realistic (not synthetic) test circuits and to draw conclusions about its performance, about the nature and magnitude of the transients associated with its application, and to evaluate the effectiveness of capacitors and diodes as surge suppressors.

3.1 Generator/Switched Motor Tests

A series motor and shunt connected generator were connected in "pump back" configuration with losses supplied from a Ward Leonard system of variable voltage for loss supply. The constants of the various machines and the CLD used are shown in TABLE 4.

TABLE 4

	<u>Generator G2</u> <u>Ward Leonard</u>	<u>Pump Back</u> <u>Generator</u>	<u>Pump Back</u> <u>Motor</u>
Make	GE	Diehl	GE
Rated Horsepower (HP)	2.5	6.1	7.5
Rated Voltage (V)	230	230	230
Armature Resistance (Ω)	0.61	0.807	0.53
Armature Inductance(H)	0.017	0.0113	0.0193
Brush Voltage Drop (V)	3	2	2
EMF - Excitation Constant (V/RPM/A)		3.37	0.053
Type of Field	Shunt	Shunt	Series
Field Resistance (Ω)		585	0.155
Field Inductance (H)			0.007

CLD Design

R = 0.01	(Radius of Bore, cm)
q = 1	(Number of Parallel Bores)
$t_v = 0.0007$	(Time to Vaporize, seconds)
$\Omega_c = 0.49$ ohms	("Cold" Resistance, ohms)
$l = 1.6$	(Bore Length, cm)
V = 200	(Rated Voltage)
I = 30	(Rated Current to Vaporize Into)
3 Atmospheres	(Pressure)

The switching system used was the system described in USBM Report #HO 357079 consisting of a tungsten electrode vacuum switch in parallel with, and used for commutating the current into, a liquid mercury filled CLD. After change of state (vaporization), the presence of full line voltage (nearly) across the CLD was utilized to trigger a thyristor which in turn opened a second, series connected vacuum switch. The overall scheme is shown in Figure 7.

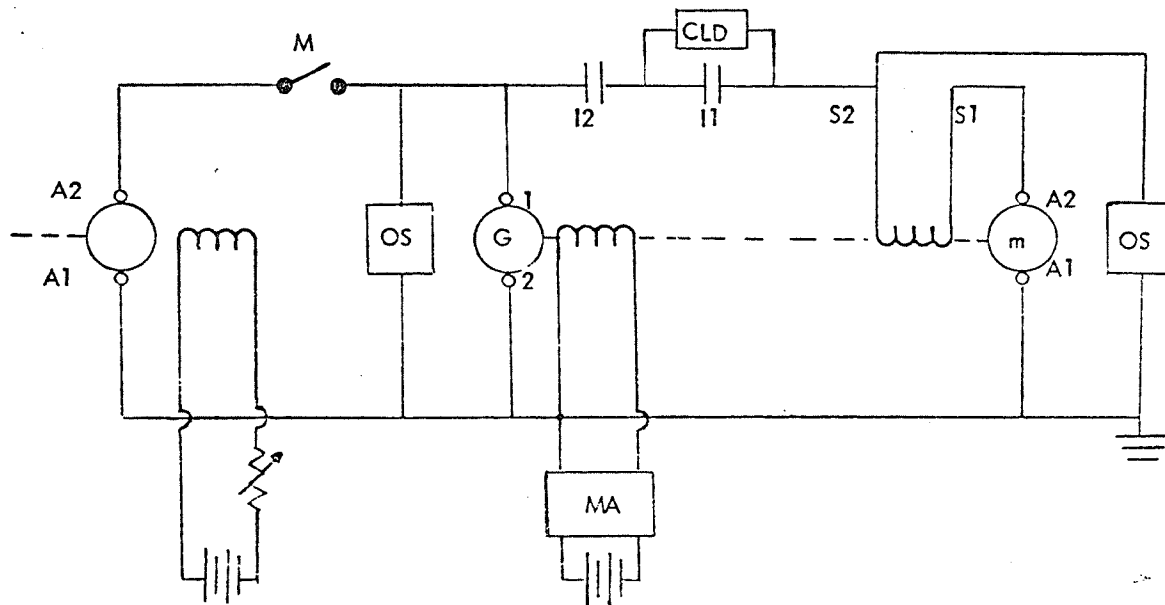


Figure 7. Circuit Used for the Pump Back Testing

M = backup contact
 I1, I2 = vacuum switches
 MA = magnetic amplifier
 OS1, OS2 = overvoltage suppressors
 S1, S2 = series field of the motor

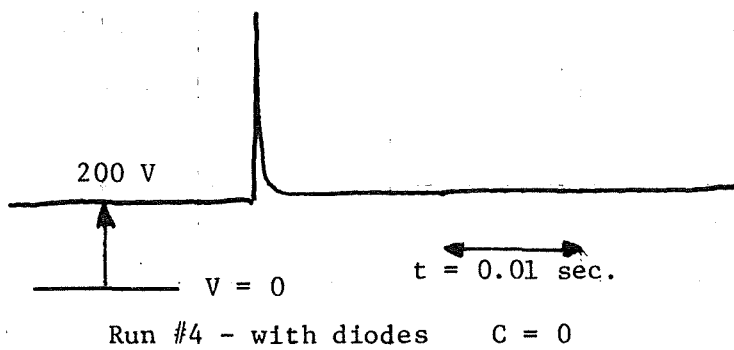


Figure 8. Generator Voltage With No Overvoltage Suppressor.

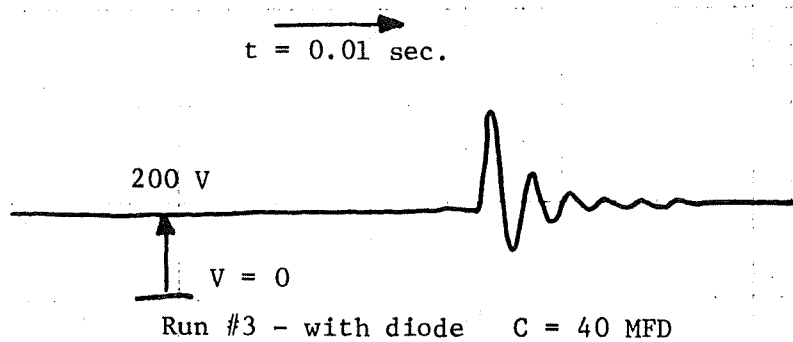


Figure 9. Generator Voltage with $40\mu\text{F}$ Parallel with the Generator.

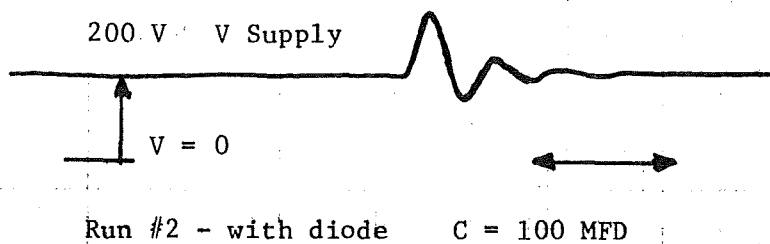


Figure 10. Generator Voltage with $100\mu\text{F}$ Parallel with the Generator.

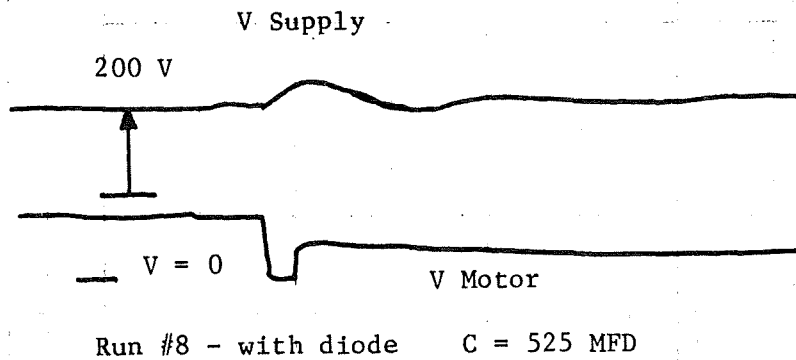


Figure 11. a) Generator Voltage with 525 μ F Parallel with the Generator.
b) Motor Voltage Clamped by the Free Wheeling Diode.

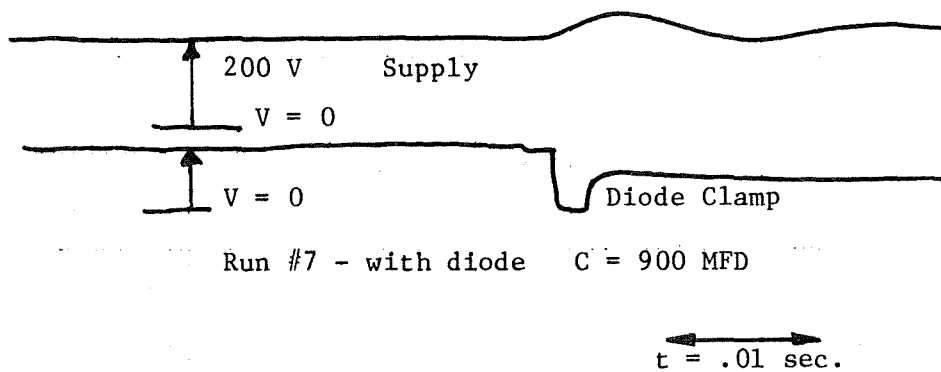


Figure 12. Motor and Generator Voltage with 900 μ F Parallel to the Generator.

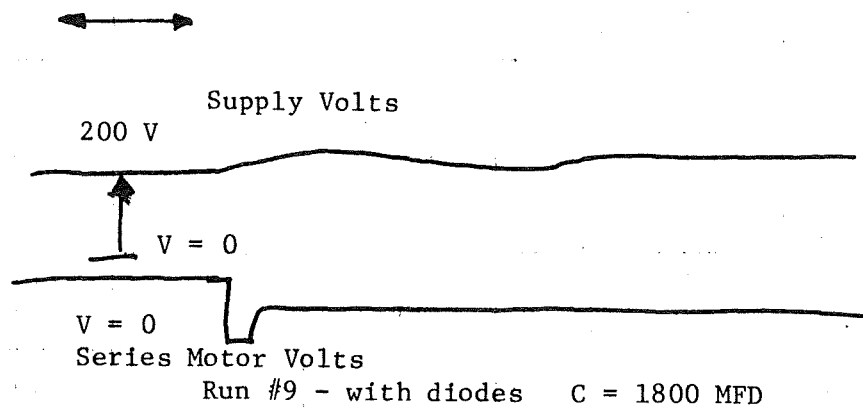


Figure 13. Motor and Generator Voltage with 1.8 μ F Parallel to the Generator.

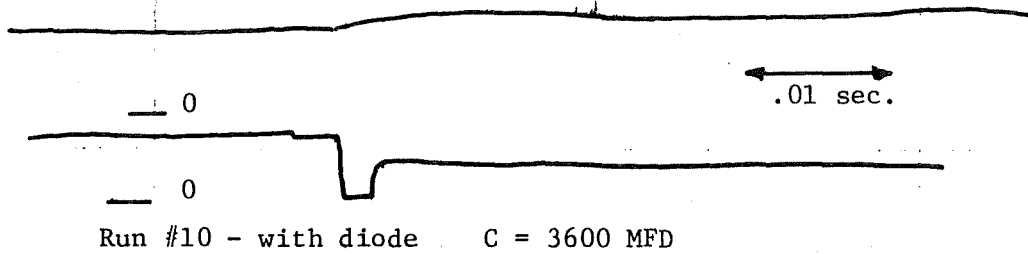


Figure 14. Generator Voltage with $3.6\mu\text{F}$ Parallel to the Generator.

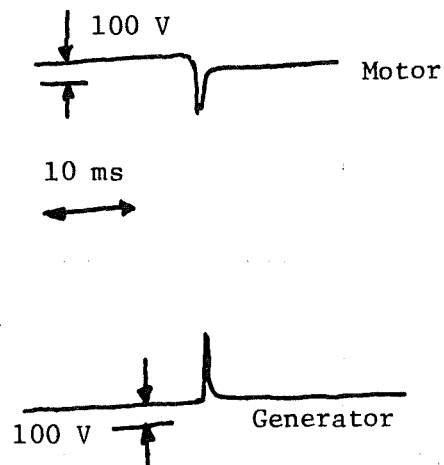


Figure 15. Pump Back System; Test No. 2/5-5-76.

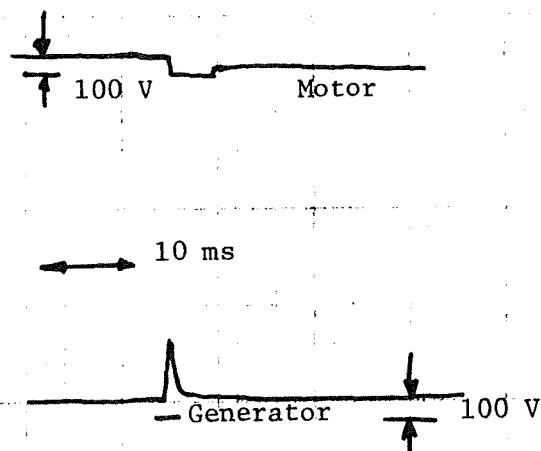


Figure 16. Pump Back System; Test No. 4/5-5-76.

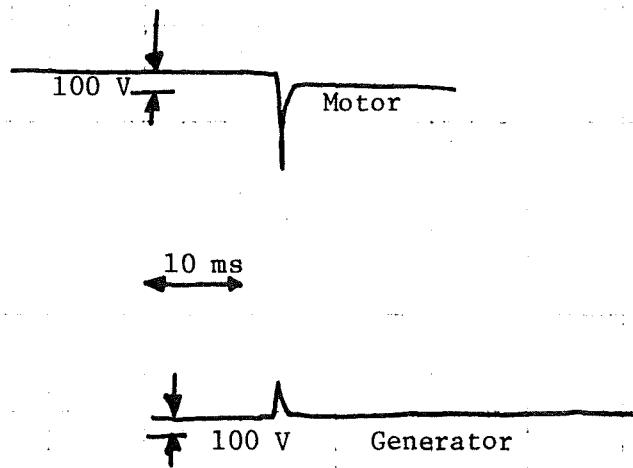


Figure 17. Pump Back System; Test No. 3/5-5-76.

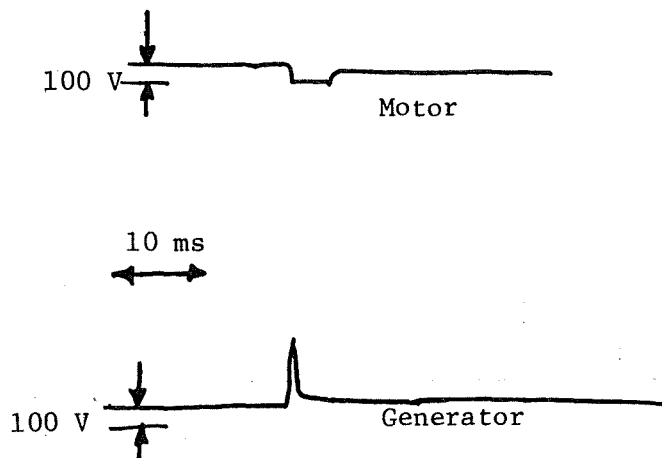


Figure 18. Pump Back System; Test No. 5/5-5-76.

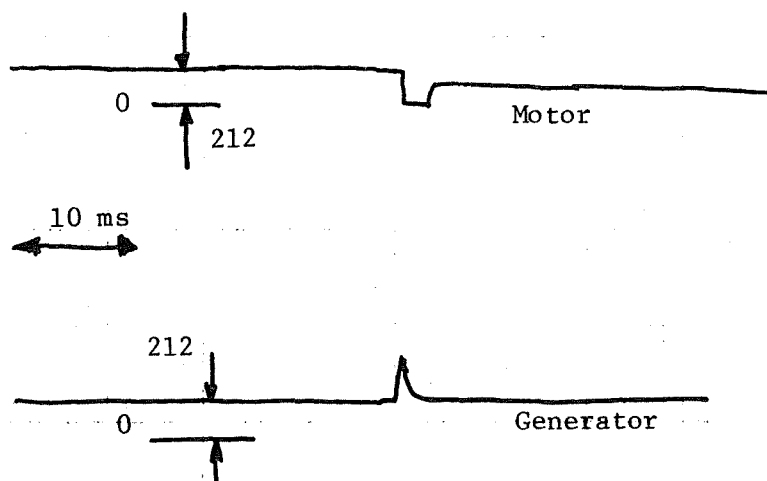


Figure 19. Pump Back System 212V Operation Diode at the Motor.

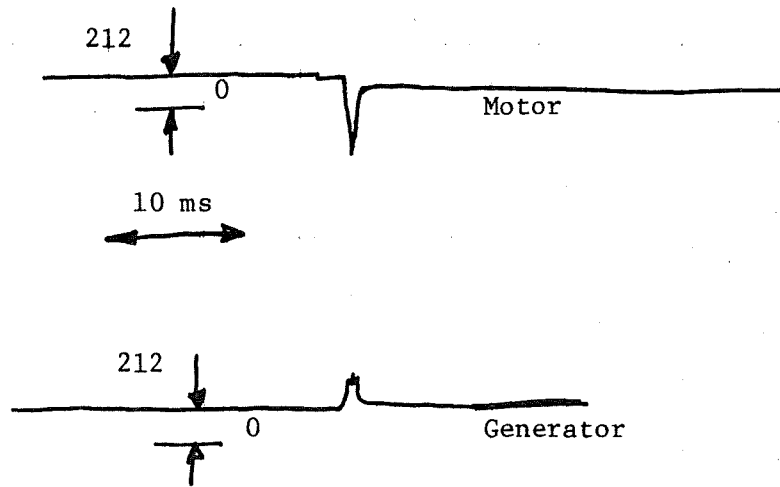


Figure 20. Pump Back System 212 V Operation;
No Diode at the Motor

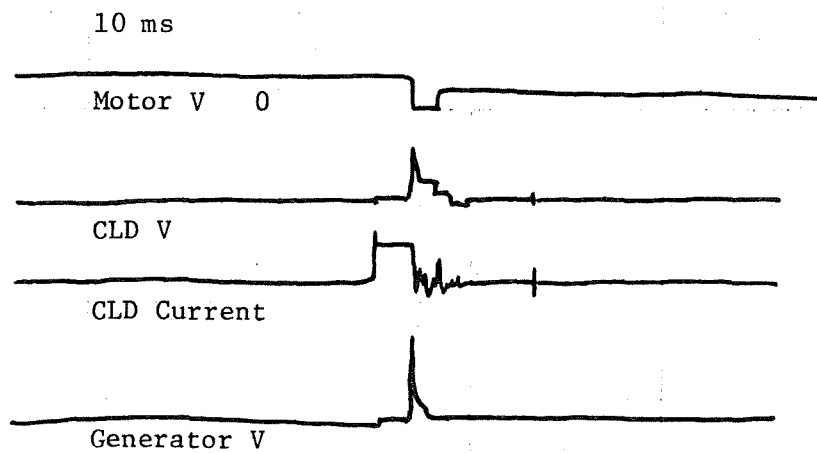


Figure 21. Pump Back System 212V Operation;
Typical CLD Voltage and Current
Oscillographs.

Operation without surge suppression yielded a strong negative voltage spike at the motor terminals, and a positive overvoltage at the generator (see Figure 8). Different methods were employed to suppress these overvoltages. A "free wheeling diode" across the motor terminals proved adequate to suppress the negative voltage spike. The voltage will drop to zero (actually the negative of the diode forward voltage drop) and as time passed, would become positive but at a value much lower than the rated voltage of the motor (see Figure 11). This technique increased slightly the positive overvoltage at the generator. A number of tests were run with capacitance. All tests were run at 200V and 24A at the motor. The recordings of the generator voltage for the cases of no generator suppressor, 40 μ F, 100 μ F, 525 μ F, 900 μ F, 1800 μ F, and 3600 μ F appear in Figures 9-14, respectively. In Figures 11-14, the motor voltage is also recorded and the action of the free wheeling diode which clamps it to zero is observable.

The simplified calculation presented in equation (3) was utilized to predict generator overvoltages to be expected with various values of shunt capacitance. TABLE 5 presents the results and a comparison of calculated and observed overvoltages as well as the overvoltage predicted by a computer model of the system. (See the following section for a discussion of the computer simulation.)

TABLE 5

Overvoltages at the Generator of the Pump-Back System Operating at 200V, 24A

<u>Added Capacitance in F</u>	<u>Measured Gen. Voltage</u>	<u>Calculated Gen. Voltage</u>	<u>Computer* Results</u>
0	660	---	664
40	450	459	457
100	365	382	375
525	275	285	282
900	269	265	264
1800	243	246	246
3600	232	233	232

Both silicon carbide and metal oxide varistors were used for generator protection in this series of tests. When they were not paralleled with capacitors, the peak voltage could be calculated from their characteristics since the initial current would be equal to the current of the inductance of the generator coils. The energy absorbed by the varistors can be calculated as the sum of the energy stored in the armature coils of the two generators, if the energy consumed on the coil resistance is neglected.

The initial peak of the voltage can be lowered if a capacitor is placed in parallel. It can absorb the initial current while the capacitor will limit the oscillation.

In Figures 15-18 four typical cases are shown. The operating voltage was 100V, the motor was receiving 21.0A, the generator was supplying 12.7A and the Ward-Leonard generator the remainder, 8.3A.

In Figure 15 no suppressors were used. The time for the CLD to operate was 3.5 ms. The negative surge of the motor was 370V and the positive surge voltage of the generator reached 463V.

In Figure 16 a diode was used at the terminals of the motor and a silicon carbide varistor (NL 9RV3A11, rated 100V DC) was placed at the terminals of the generator. The arc in the CLD was unstable, which lowered the transient overvoltage at the generator and increased the amount of energy dissipated in the bore wall area of the CLD. At the motor, the diode clamped the voltage essentially to zero.

In Figure 17 the test of Figure 15 is repeated. The effects of the unstable arc are clearer here.

In Figure 18 no suppressors were used at the generator. The diode of the motor caused the generator voltage to jump to 450V in spite of the unstable arc.

In Figures 19, 20, and 21, the results of two more typical cases are displayed. The voltage, at steady state was 212V; the motor was receiving 26.5A, the generator was supplying 18A and the Ward-Leonard generator the remaining. The system was operating at 1800 RPM. In Figure 19 a diode was used at the motor and a metal oxide varistor (GE MOV V250DA40A, rated 330V DC) was placed at the terminals of the generator. The generator voltage peak reached 500V.

The interruption and restriking of the arc in Figure 20 limited the voltage of the motor to 300V and that of the generator to 380V, though no suppressors were used.

In Figure 21, the voltage across the CLD and the current through it are shown for the case of multiple arc restriking.

3.2 Computer Simulation of the System

It appeared desirable, for future application, to develop a computer model of the pump back loading system, with its nonlinearities and any of the various nonlinear surge suppression schemes that might be used or considered for potential usage. This section describes the model and the program that was written and presents the results for various schemes.

The program was written in CSMP* and is defined by the block diagram of Figure 22. The transient equations of the dc machines are used and friction and inertia of the rotating parts are included. The integration method utilized was the Fourth Order Runge-Kutta with variable integration step.

* Continuous System Modelling Program.

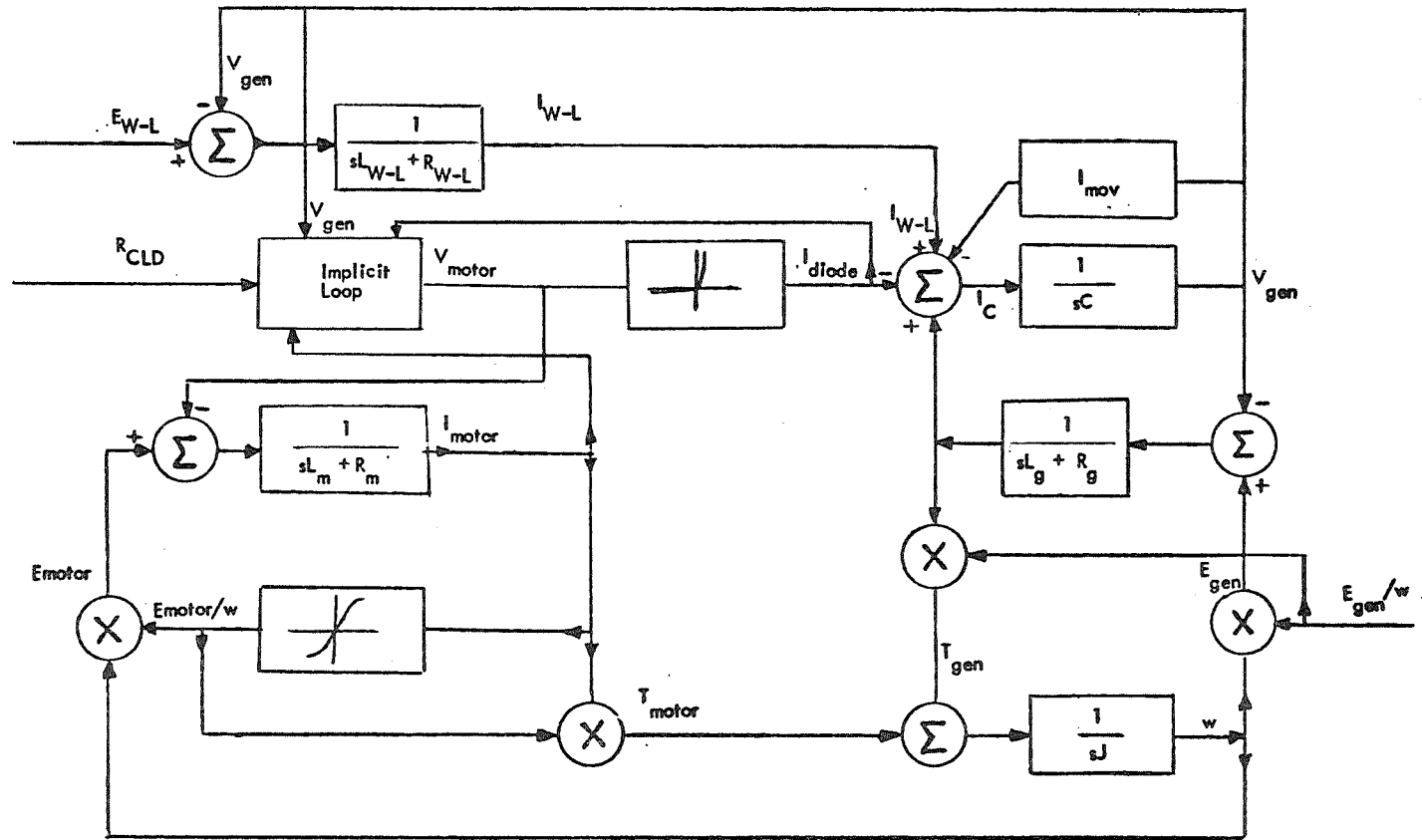


Figure 22. Block Diagram for the Simulation of the Pump Back System

The steady state parameters were calculated with a simple Gauss iterative scheme, a flow chart of which appears in Figure 23. Other supporting sub-programs were also used. They are:

- (a) The calculation of the current of the diode across the motor.
- (b) A linear interpolation for the voltage versus current of the motor.
- (c) The friction torque as a function of revolutions per minute.
- (d) The current of the varistor versus voltage.

A complete listing of the program follows.

The program was run for a variety of surge suppressing schemes, voltage and current levels. Figures 24-30 show the generator overvoltages when the motor, running at 200V, 24A, was switched, both without the use of suppressors, and for 400 μ F, 100 μ F, 525 μ F, 900 μ F, 1.8mF and 3.6mF. These results agree quite well with the test results appearing in Figures 8-14 (see also TABLE 5). In Figure 31 and 32 the generator voltage is shown for the condition when the motor is loaded to 212V, 26.5A and 100V, 21A respectively before switching. Overvoltages without a suppressor and with a suitable metal oxide varistor are plotted. A small capacitor is placed parallel to the varistor for the purpose of absorbing the initial current of the generator armature coil.

The tests with the pump back configuration gave realistic results and increased the confidence in the CLD design method, the switching scheme and the control and monitoring configuration. However, prior to field tests, a better understanding of two additional aspects was needed, i.e.,

- (a) The behavior of rectifier type power supplies instead of generators, during switching surges.
- (b) The behavior of the CLD in high current situations.

With respect to (b), tests were conducted as reported in the Final Report in USBM #357079 but it was considered important that these tests be repeated with solid state rectifiers.

To accomplish this, a three phase, full wave rectifier (a welding transformer) was employed. Its DC terminals were short circuited rather than connected to an inductive load. This was the main drawback of this configuration. The test set up consisted of a three phase transformer with variable leakage impedance, which was originally used for an arc welder; a three phase full wave rectifier short circuited through the CLD assembly and a current measuring shunt resistor; and a control circuit. A schematic of the configuration appears in Figure 33.

- (a) The leakage reactance of the transformer was adjusted so that the short circuit direct current would be 200A. At this setting the transformer parameters were measured or calculated.

Primary line to line voltage: 240V
 Secondary line to line voltage: 59V
 Total resistance referred to the secondary: .0125 Ω
 Leakage reactance referred to the secondary: 89.1 x 10⁻⁶ H

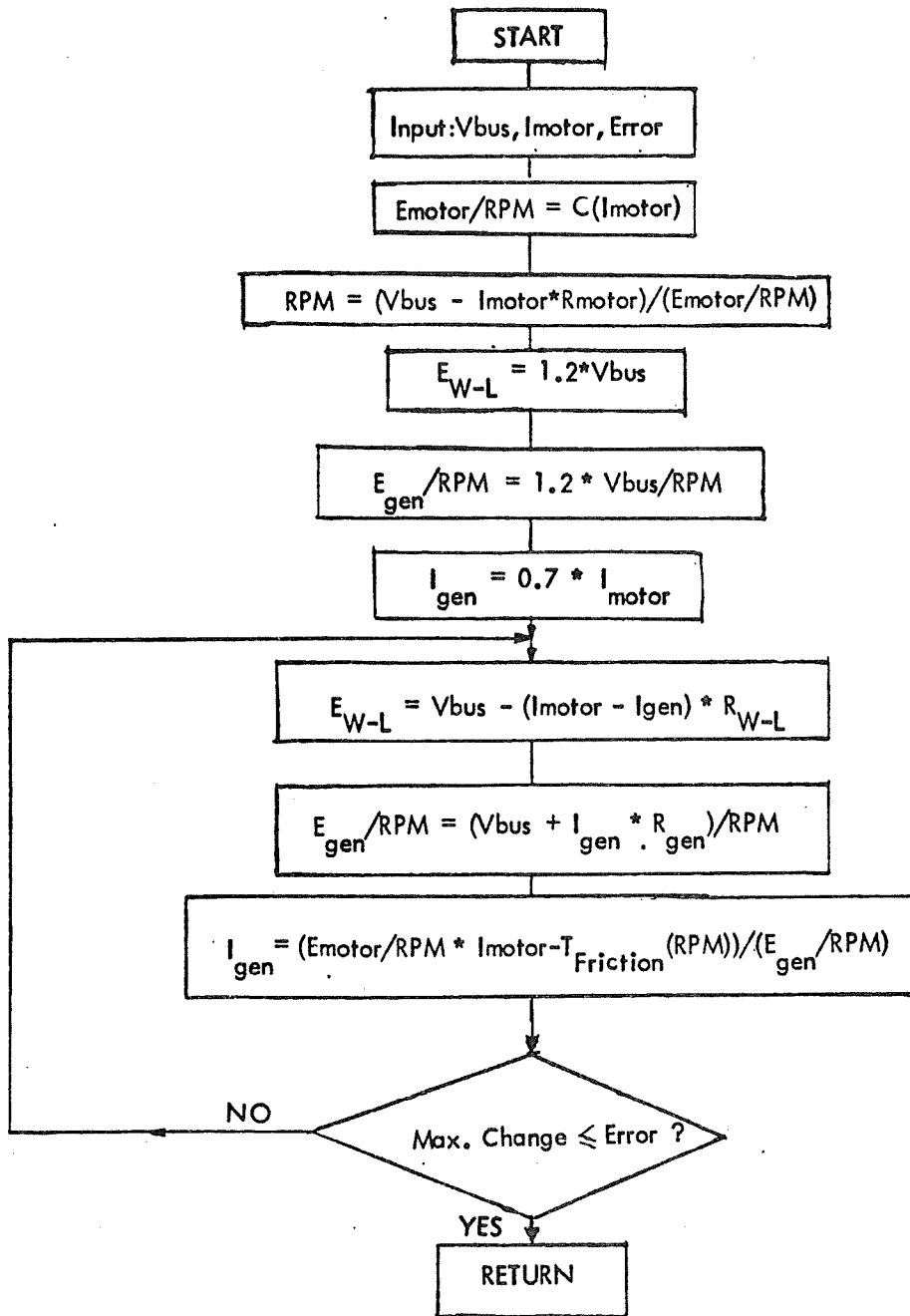


Figure 23. The Flow Chart for the Subroutine that Calculates the Steady State Parameters of the Pump Back Systems.

MAIN PROGRAM IN CSMP

```

MACRO XX=VMM(VG,I3,ZZ)
  VL=-5.
  VN=IMPL(VL,.001,VM1)
  ISUPM=IDIODE(VN)
  VM1=VG-(I3+ISUPM)*ZZ
  XX=VN
ENDMACRO
INITIAL
STORAGE AI3(20),AE3(20)
TABLE AE3(1-5)=0.,6.67E-2,8.89E-2,1.078E-1,1.3E-1,...
      AI3(1-5)=0.,10.,15.,20.,27.5
CONST R1=.61,R2=.807,R3=.658,J=.1559,...
      L1=.017,L2=.0113,L3=.0193,...
      C12=3.6E-3
PARAM V1=200.,I30=24.,...
      ERR=.0001,...
      Z1=.48,Z2=200.0
      P1=L1/R1
      P2=L2/R2
      P3=L3/R3
      E1,W0,I20,E220,E330=STEADY(R1,R2,R3,V1,I30,ERR,AE3,AI3)
      E20=E220*W0
      E30=E330*W0
      I10=I30-I20
DYNAMIC
      I22=(E220*W-VG)/R2
      I2=REALPL(I20,P2,I22)
      I33=(-E33*W+VM)/R3
      I3=REALPL(I30,P3,I33)
      E33=C(AE3,AI3,I3)
      SW=(E33*I3-E220*I2-FRICT(W)/W)/J
      W=INTGRL(W0,SW)
      ZZ=Z(Z1,Z2,TIME)
      I11=(E1-VG)/R1
      I1=REALPL(I10,P1,I11)
      VM=VMM(VG,I3,ZZ)
      ISUPM=IDIODE(VM)
      ISUPG=I1+I2-I3-ISUPM
      IC=ISUPG
      VG=INTGRL(V1,IC/C12)
TERMINAL
TIMER FINTIM=2.E-2,OUTDEL=.4E-4,PRDEL=2.5E-4,DELMIN=1.5E-10
PRTPLT VM,VG
PREPAR VG,VM
END
STOP

```

SUBROUTINE STEADY FOR THE CALCULATION OF THE
STEADY STATE OPERATION OF THE PUMBACK SYSTEM

```

SUBROUTINE STEADY(R1,R2,R3,V1,I30,ERR,AE3,AI3,E10,W0
1,I20,E220,E330)
  DIMENSION AE3(20),AI3(20)
  REAL I20,I30,I2H,I10
  E330=C(AE3,AI3,I30)
  W0=(V1-I30*R3)/E330
  E10=1.2*V1
  E220=1.2*V1/W0
  I20=.7*I30
1  E1H=E10
  E10=V1+(I30-I20)*R1
  E2H=E220
  E220=(V1+I20*R2)/W0
  I2H=I20
  I20=(-FRICT(W0)/W0+E330*I30)/E220
  X=AMAX1(ABS((E1H-E10)/E10),ABS((E2H-E220)/E220),
1ABS((I2H-I20)/I20))
  IF(X.GE.ERR) GOTO 1
  I10=I30-I20
  E1=E10
  W=W0
  E30=E330*W0
  E20=E220*W0
  WRITE(6,4)
  WRITE(6,2)R1,R2,R3,L1,L2,L3
  WRITE(6,3) E1,E20,E30,I10,I20,I30,W,V1
4  FORMAT (1H1,45X,'INITIAL CONTITIONS')
2  FORMAT(1H/,30X,'R1='F12.5,5X,'R2='F12.5,5X,'R3='F12.5,/
1,1H ,30X,'L1=' ,F12.5,5X,'L2=' ,F12.5,5X,'L3=' ,F12.5,5X)
3  FORMAT(1H ,30X,'E1=' ,F12.5,5X,'E2=' ,F12.5,5X,'E3=' ,F12.5,/
1,1H ,30X,'I1='F12.5,5X,'I2=' ,F12.5,5X,'I3=' ,F12.5,/
2,1H ,45X,'W='F12.3,5X,'V1=' ,F12.5,/)
  RETURN
  END

```

GE MOV CURRENT VERSUS VOLTAGE

```
FUNCTION IMOV(V)
REAL IMOV,I
V1=ABS(V)
IF(V.LE.304.36)GO TO 1
I=EXP(-163.444+ALOG(V1)/.036)
IMOV=I*SIGN(1.,V)
RETURN
1 IMOV=V/30436.
RETURN
END
```

DIODE CURRENT VERSUS VOLTAGE

```
FUNCTION IDIODE(VM)
REAL IDIODE
IF(VM+.65) 2,2,1
1 IDIODE=0.
RETURN
2 IF(VM+.925) 4,4,3
3 IDIODE=(VM+.65)/5.5
RETURN
4 IDIODE=(VM+.925)/0.5-.05
RETURN
END
```

LINEAR INTERPOLATION FOR THE CHARACTERISTIC
OF THE MOTOR

```

FUNCTION C(AE3, AI3, XI3)
DIMENSION AE3(20), AI3(20)
DO 3 I=1, 20
IF (ABS(XI3)-AI3(I))1, 2, 3
3 CONTINUE
2 C=AE3(I)*SIGN(1., XI3)
RETURN
1 C=(XI3-AI3(I))/(AI3(I-1)-AI3(I))*(AE3(I-1)-AE3(I))+AE3(I)
1*SIGN(1., XI3)
RETURN
END

```

FRICION POWER AS A FUNCTION OF RPM

```

FUNCTION FRICT(W)
W1=ABS(W)
IF(W1.LE.275.)GO TO 1
FRICT=-129.553+.4712*W1
RETURN
1 FRICT=0.
RETURN
END

```

THE CLD RESISTANCE AS A FUNCTION OF TIME

```

FUNCTION Z(Z1, Z2, TIME)
IF(TIME-.001)1, 1, 2
1 Z=0.
RETURN
2 IF(TIME-.003)3, 3, 4
3 Z=Z1
RETURN
4 Z=Z1+Z2*(TIME-.003)/.001
RETURN
END

```

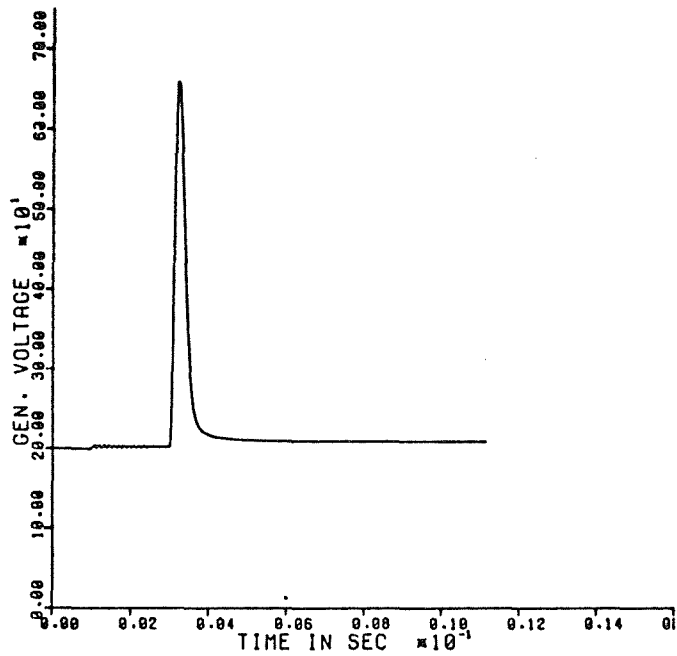


Figure 24. Generator Voltage 200V, 24A Operation
No Suppressors

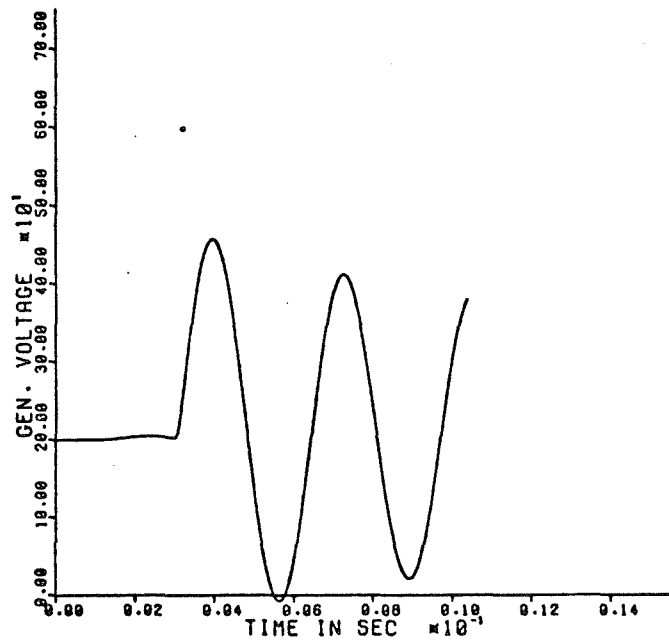


Figure 25. Generator Voltage 200V, 24A Operation
40µF at the Generator

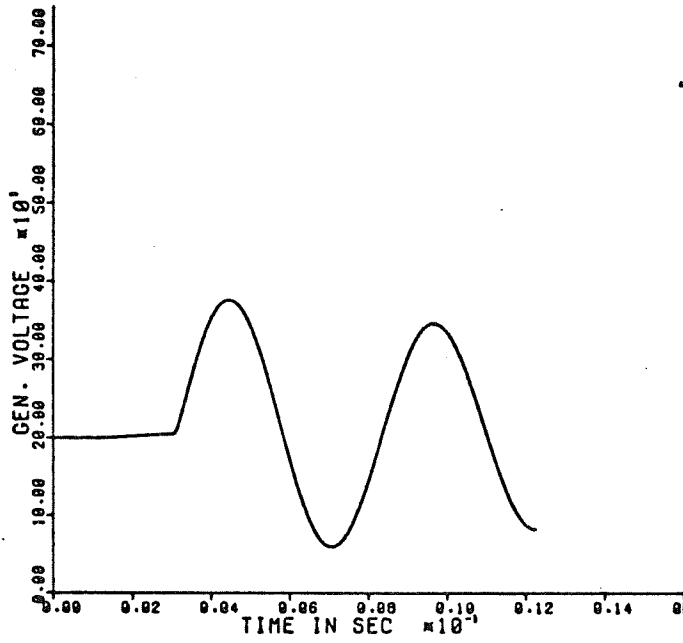


Figure 26. Generator Voltage 200V, 24A Operation
100 μ F at the Generator

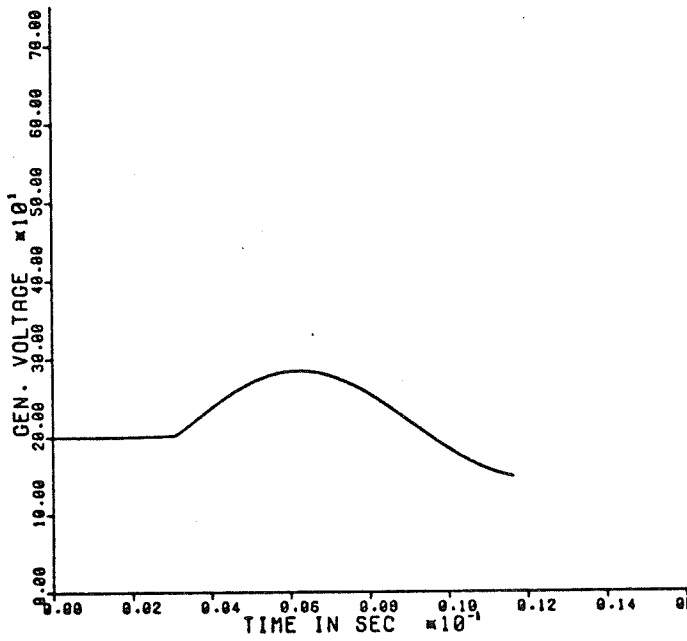


Figure 27. Generator Voltage 200V, 24A Operation
525 μ F at the Generator

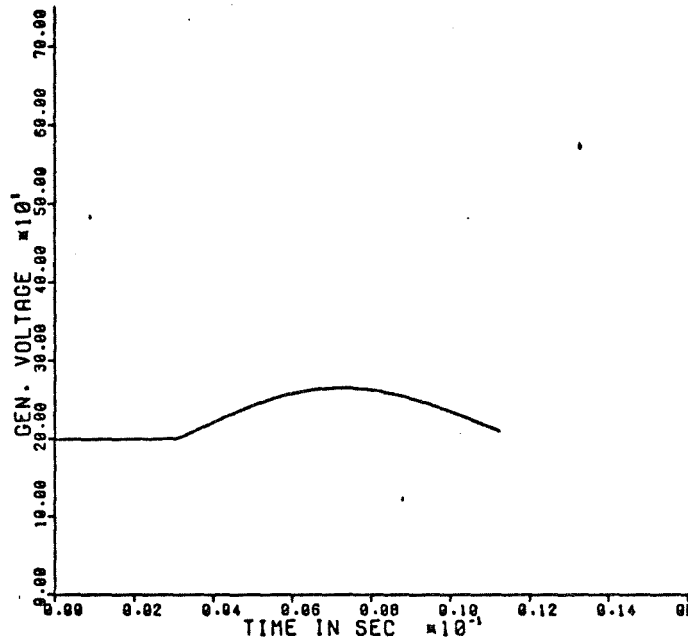


Figure 28. Generator Voltage 200V, 24A Operation
900µF at the Generator

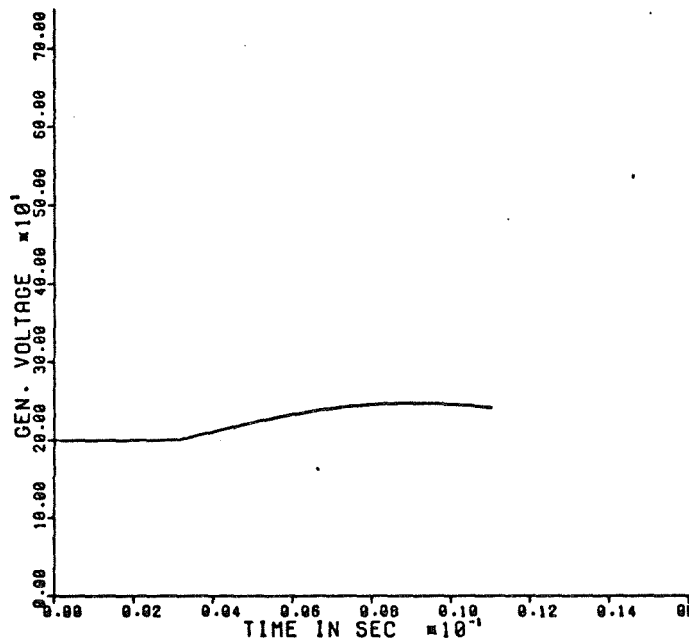


Figure 29. Generator Voltage 200V, 24A Operation
1800µF at the Generator

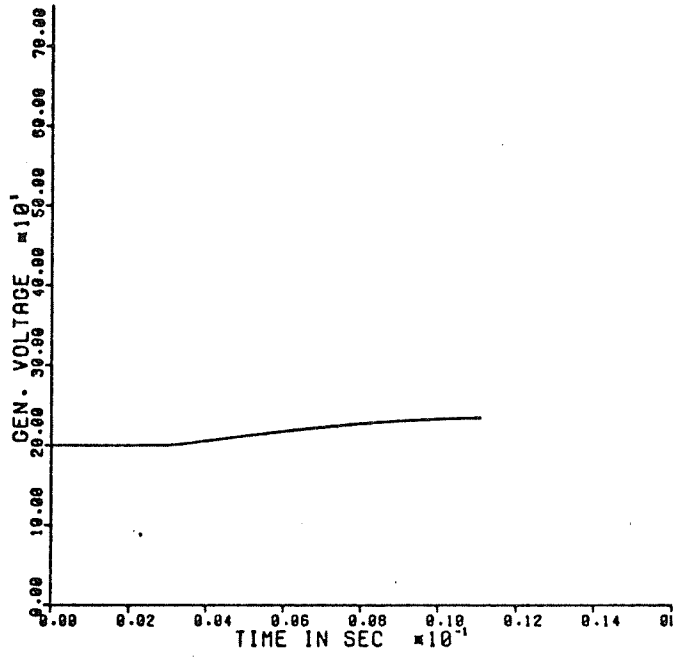


Figure 30. Generator Voltage 200V, 24A Operation
3600 μ F at the Generator

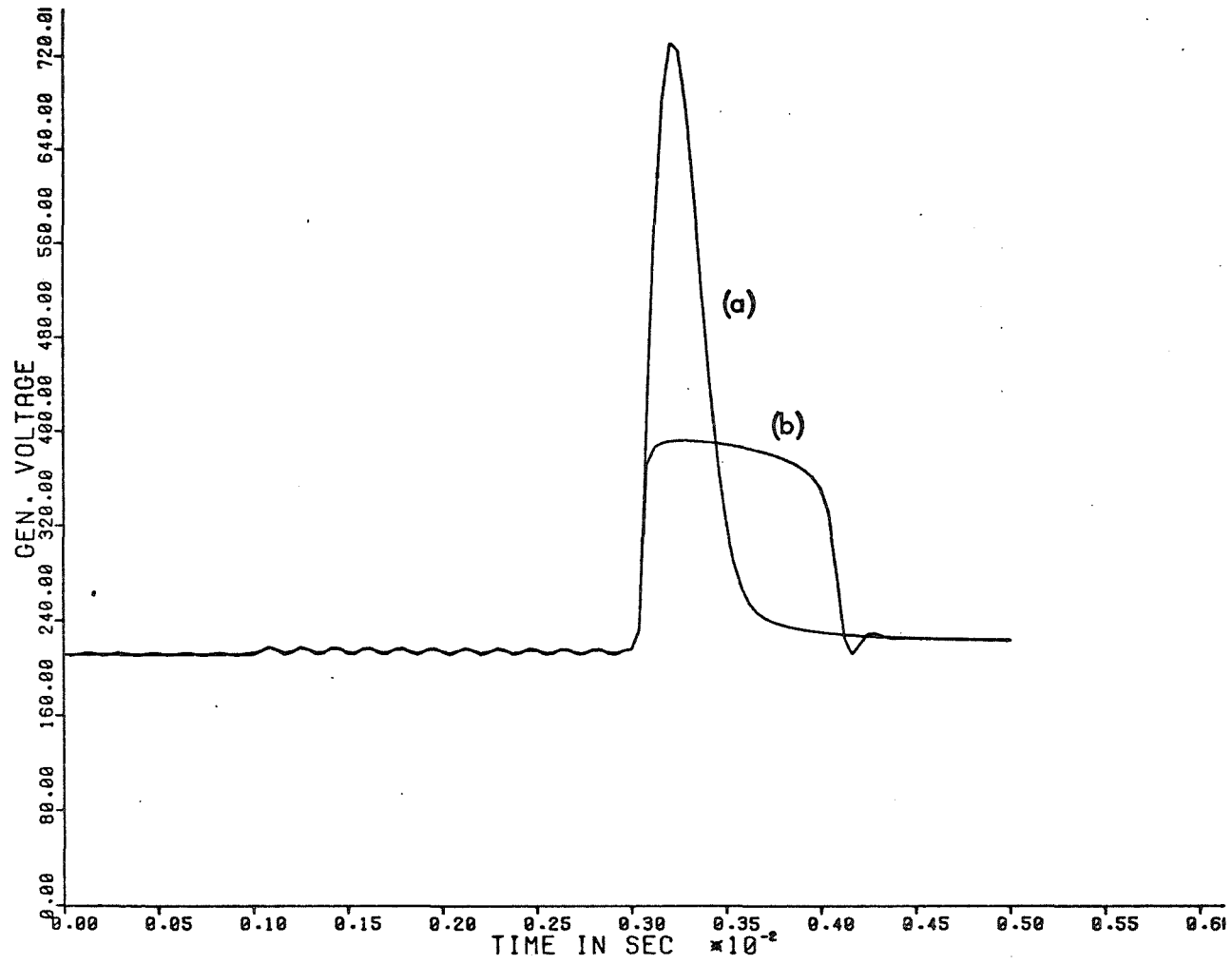


Figure 31. Generator Voltage of the Pump Back System. Operation at 212V, 26.5A.
 (a) without varistor
 (b) with varistor

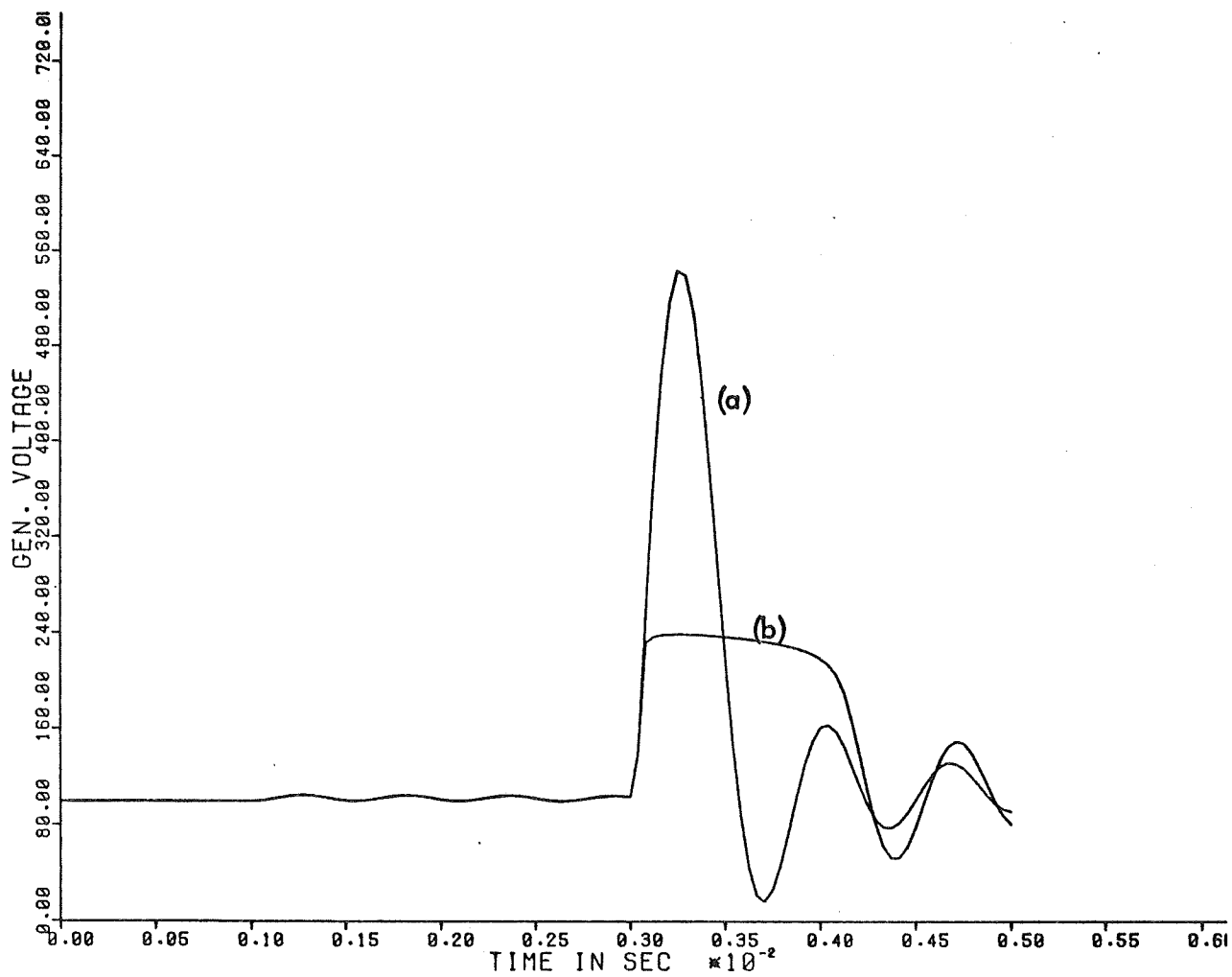


Figure 32. Generator Voltage of the Pump Back System. Operation at 100V, 21A.
 (a) without varistor
 (b) with varistor

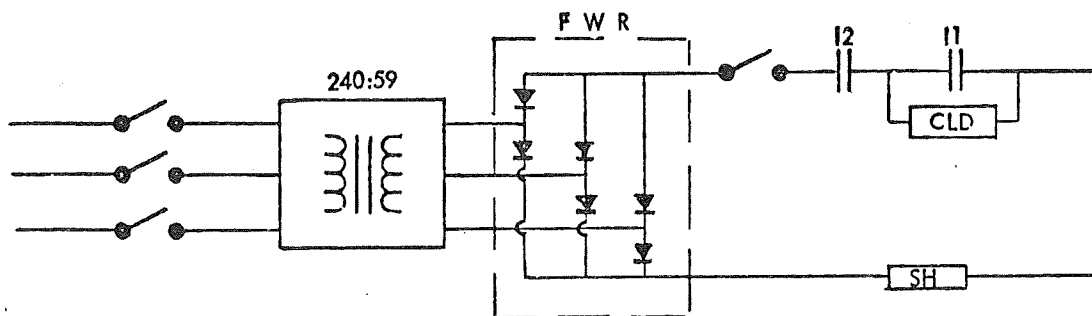


Figure 33. The Configuration for the Short Circuited Rectifier

FWR Full Wave Rectifier
 I1, I2 Vacuum Breakers
 SH Current Measuring Resistor

The primary voltage actually applied was 212V line to line, resulting in a secondary voltage of 52.3V.

- (b) The full wave rectifier consisted of diodes rated 1000V RPV placed two in series to achieve an RPV rating of 200V.

DC voltage: $1.35 V_{LL} = 70.6V$

Peak reverse voltage: $2 \times V_{LL} = 104.6V$

- (c) The CLD design parameters were:

Radius: 0.05 cm, single bore

Length: 2.25 cm

Pressure: 3 Atmospheres

The CLD was designed for an open circuit voltage of 70V, 1.5 milliseconds to vaporize, at 200A and with a resulting conductivity (average) 15Ω cm after vaporization. The material used was Alumina (Al_2O_3) bores cast in Sauereisen 8X with monaluminum phosphate.

In the tests no automatic removal of the CLD took place after vaporization and as a result it was left in the circuit for time periods of seconds rather than milliseconds, and multiple arc interruptions and restrikes occurred. As shown in Figure 34, with each restrike the capacitor voltage increased and was trapped by the diodes. Since the next overvoltage occurred very quickly, the voltage of the capacitor didn't have time to drop by bleeding through the parallel resistor, and therefore the next charging started from the previous voltage. This eventually decreased the ability of the surge suppressors to absorb energy of transients resulting from restriking. It also precluded making accurate measurements of surge levels.

These were run for different values of capacitor. When these values were 7.2, 5.4 or 3.6mF the results were satisfactory, but when the suppressing scheme was accidentally removed one of the diodes of the rectifier failed. The results of this series of tests were not considered satisfactory because of the length of time the CLD was in the circuit and the nature of this rectifier configuration (a welding transformer).

However, it did point up the need for speedy disconnection of the circuit when the CLD is used for switching or fault current limiting.

In summary, the lab tests, the simplified calculation procedure and the simulation model did give confidence in our ability to predict and control electrical transients associated with high speed switching and interruption of heavy current.

4.0 CLD DESIGN FOR FAULT CURRENT LIMITING

Fault current limiting is a complex task regardless of what method is used to achieve the limiting. The problem, overall, consists of three distinct areas; two of which are easily resolved. The other is a formidable problem and was not attached directly in this research. The three problem areas are:

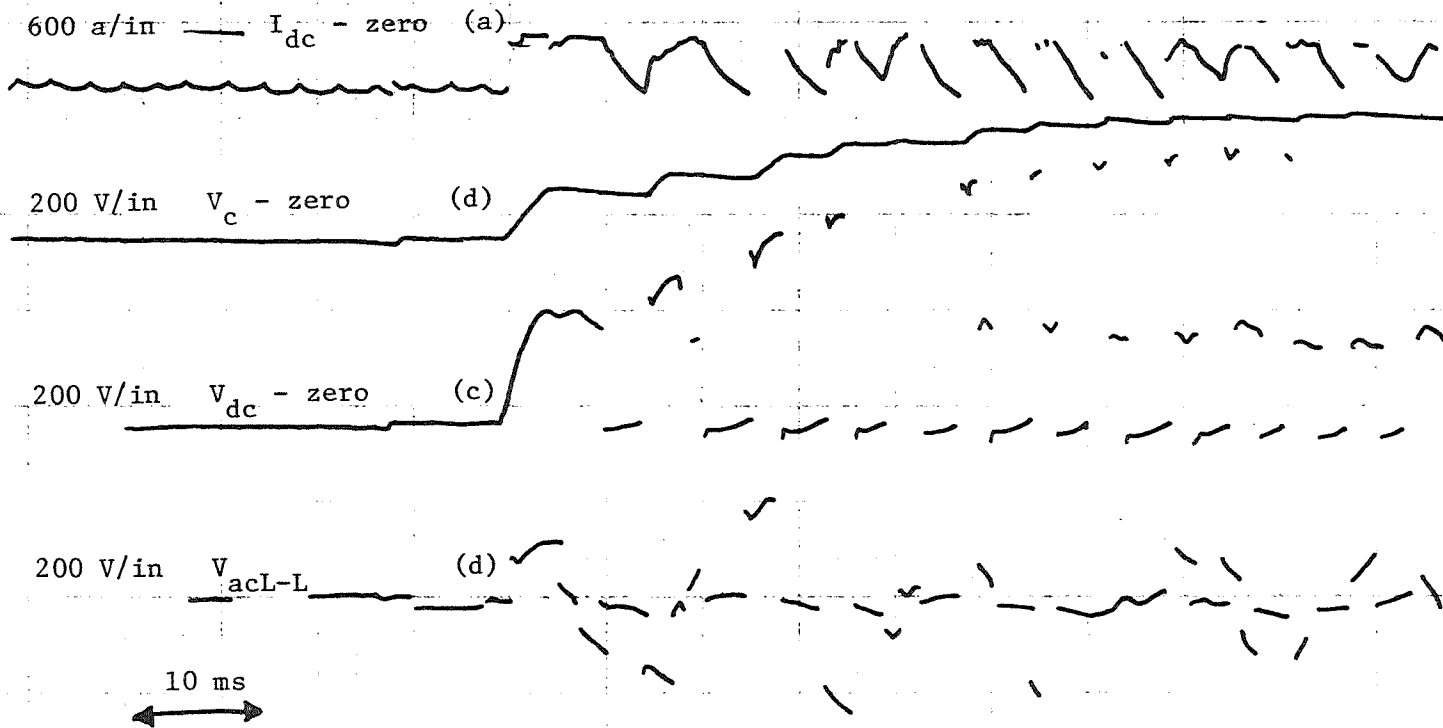


Figure 34. Short Circuited Rectifier Test

- a) DC Current
- b) Capacitor Voltage
- c) DC Voltage
- d) Line to Line Voltage

1. detection of the presence of the fault;
2. insertation of a fault current limiter (CLD);
3. design of the CLD.

In this section a discussion of each of the above problem areas is presented.

4.1 Detection of the Presence of the Fault

Faults can occur anywhere on the system. If faults occurred only at the terminals of the rectifiers, or supply, detection could be achieved based on rate of rise of fault current, because a predictable amount of inductance is present and the rate of rise of fault current can be calculated, or closely estimated. However, if the fault occurs a substantial distance from the rectifier terminals, the inherent inductance (estimated at 0.4 microhenry per foot) is present and rate of rise of current on fault may be the same order of magnitude as the rate of rise of current for a highly (relative) inductive load, such as a trolley motor, close in to the rectifier terminals. Further compounding the problem is that the close in fault may be a high resistance fault and the resulting fault current may be as low as, say, 100 amperes which is not damaging to the supply equipment but which may pose a safety hazard, i.e., fire. If detection on rate of rise is attempted, it should be noted that the di/dt associated with mine electrical loads and faults varies between 200,000 and 10,000,000 amperes/sec., depending on the amount of inductance present. For a low grade fault, for example 100 amperes maximum, time for detection based on di/dt is thus seen to be between 10 and 50 microseconds! Detection based on absolute fault current level is not reliable because of the problem of distinguishing between normal high value inrush current and the low fault current level associated with high resistance faults. Lack of a suitable, reliable fault detection means will be the major obstacle to overcome in fault limiting.

4.2 Insertion of the CLD

Insertion of a fault current limiter (CLD) is easily accomplished on a rapid insertion basis using a switch actuated by an "Exploding Bridgewire Detonator" (EBD). An EBD is a device similar to a blasting cap but differing in that the firing pulse required is so unique that accidental firing is not possible (as in a conventional blasting cap). The general order of magnitude of the firing pulse is the discharge of a 1 microfarad capacitor charged to 2000 volts; yielding a 1000 ampere, 1 microsecond pulse. The resulting detonation velocity is in the range 5000-8000 meters per second and can be used to move a piston and switch contacts immersed in oil.

Discussions were held with representatives of Reynolds Industries, Inc., 5005 McConnell Avenue, Los Angeles, California, 90066 (212-823-5491). They felt a multiple detonator (for 4 operations) could be built which would have the following characteristics (as a switch):

Dimensions: Approximately 3 x 7.25 inches
 Developed Arc Voltage: 300
 Continuous Current: 1000 amperes (1.5 square inch contact area)

Contact Travel: 0.25 inch
 Contact Opening Time: 0.5 milliseconds maximum after fire command
 Contact Reclosure Time: 2 seconds, minimum

Using such a switch, current could be commutated into a CLD very quickly, and allowing the following additional time delays:

Fault Detection: 0.25 milliseconds
 CLD Vaporization: 0.25 milliseconds

total time lapse from fault to fault limit would be less than 1 millisecond.

4.3 Design of a Fault Limiting CLD

To design a CLD for this application it is necessary to know, or specify a rate of rise of current after the CLD is inserted. Accurate calculation of fault current on a rectifier is a very complex procedure and not well documented. One approach used is to calculate the inductance between source and fault and divide this into the prefault DC voltage.

This simplistic approach results from viewing the source, through the rectifier, to the point of fault as an R, L circuit, taking the derivative of the current at time zero and assuming that this rate of rise continues at a constant rate. In view of the widely variable fault possibilities, use of the simple expression for fault current rate of rise appears justifiable.

A simplified test on short circuit current limiting was conducted at the USBM, Bruceton, Pennsylvania facility and is described in Chapter 5.

5.0 FIELD TESTS

The final stage of this project, the field tests, was conducted at the experimental facilities of the U.S. Bureau of Mines at Bruceton, Pennsylvania. The apparatus used consisted of a locomotive running on a track, powered through trolley wire from a 300V, 1000A, 3 phase, full wave rectifier. Figure 35 shows schematically the electric circuit.

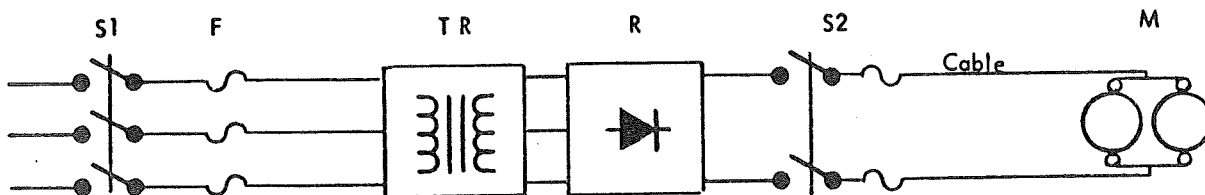


Figure 35. The Electric Circuit in the USBM Facilities at Bruceton.

S1 = load break switch
 S2 = fused disconnect switch
 F = 150A, 5.5KV fuses
 TR = 315 KVA, 3 ϕ , 60 Hz transformer 2300 Δ - 222 Δ
 R = 300 KW, 3 phase full wave rectifier
 M = locomotive motors

The locomotive had two identical DC series motors rated 300V, horsepower rating unknown, each drawing about 100 amperes at empty locomotive load. Various load conditions could be achieved by operating the locomotive up or down a grade and by applying the brakes while accelerating.

Two series of tests were conducted. The first involved the interruption of load current of the locomotive, while it was running under various load conditions. In the second, the CLD was used to limit currents on the trolley system under short circuit conditions.

5.1 Interruption of Load Current

In this series of tests the interrupting scheme was connected between the rectifier and the trolley wire from which the locomotive was powered. Before the tests took place, the surge suppressor scheme was tested by energizing and de-energizing the primary of the transformer and recording the DC voltage.

The Surge Suppressing Scheme

This was essentially the same as the one used in the laboratory for the short circuited rectifier and as described in Section 4.2. The capacitor was connected directly to the DC circuit, instead of to a separate full wave rectifier. The total capacitance used was 3600 μ F. The GE MOV varistors used were rated 250V AC, 40 joules.

Prior to the operation of the CLD, the transformer was energized and the DC voltage recorded. Figures 36 and 37 show this voltage for both the case where the capacitors and varistors were used and the case where no suppressors were employed. In the first case, the initial voltage overshoot was 17% over the steady state value; while in the second, the voltage reached 167% of its rated value.

The CLD and the Switching Scheme

The mercury filled CLD that was used for the interruption of the motor current was designed for 300V, 200A with the following characteristics:

$$\begin{aligned} R &= 0.025 \text{ cm, length} = 4.6 \text{ cm} \\ q &= 2 \text{ parallel bores of alumina} \end{aligned}$$

Calculated performance:

$$\begin{aligned} t_v &= 0.0025 \text{ millisec} && \text{(Time to Vaporize)} \\ R_c &= 0.112 \text{ ohms} && \text{("Cold" Resistance)} \\ E &= 65.3 \text{ volts/cm} && \text{(Field Intensity)} \\ ER &= 1.63 \text{ volts} \\ \sigma &= 27.5 \text{ (ohm-cm)}^{-1} && \text{(Vaporized Conductivity)} \\ R_v &= 42.6 \text{ ohms} && \text{(Vaporized Resistance)} \end{aligned}$$

An outline drawing of the CLD used is presented in Appendix B.

The connection of the cable coming from the power supply to the trolley wire was interrupted and the switching scheme was inserted as shown in Figure 38.

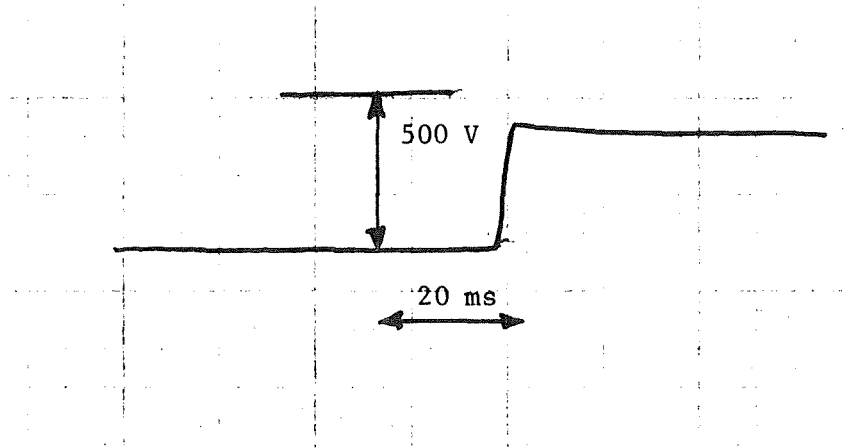


Figure 36. DC Voltage After the Energizing Transformer, 3600 μ F Across the Rectifier.

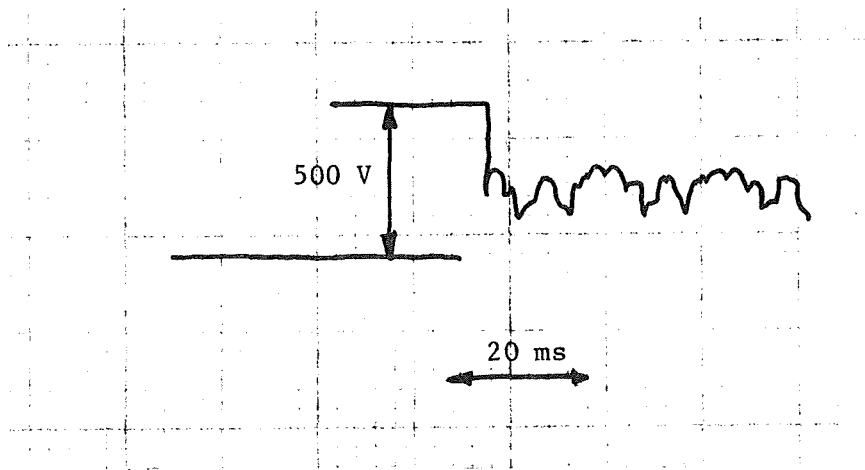


Figure 37. DC Voltage After Energizing the Transformer, No Suppressors Used.

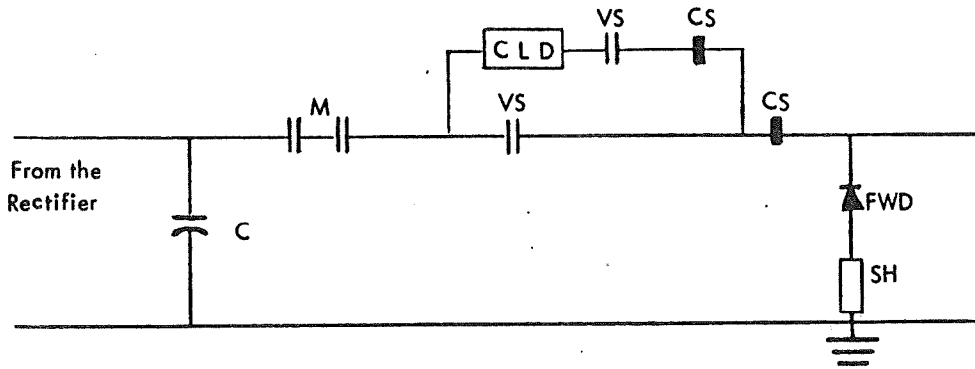


Figure 38. The Electrical Connections of the CLD for the Field Tests.

- M = back up switch
- VS = vacuum switch
- CS = current sensor
- FWD = free wheeling diode
- SH = current shunt for free wheeling diode current

The current was measured with current sensors rated 0-500A DC with accuracy of $\pm 1\%$ full scale. The control circuit was that shown in Figure 39, with small alterations for the supply of the solenoid of M, adjustments of timing relays and the setting of the voltage divider. The voltages of the supply and of the load, the current through the CLD, the current through the diode and the current of the supply were monitored on a light beam type strip chart recorder.

Test Results

Tests were conducted for various values of the current drawn from the motors. Operating time for the CLD was approximately 3 milliseconds. Figures 40, 41 and 42 depict voltages and currents when the load current was switched using the CLD. In each case successful interruptions resulted, although arc restrikes are apparent in each test. In Figure 42 it can be seen that not all of the motor current was transferred from the paralleled V.S. to the CLD. Examination after the test indicated that one of the two parallel bores was blocked by contamination, causing a doubled value of cold resistance of the CLD and the increased resistance times the total current to be commutated was in excess of the arc voltage that could be developed by the vacuum switch. Hence, total current transfer was not accomplished in that test.

Arc extinction and restrike, and accompanying 1 millisecond current pulses resulted, it is believed, from an excessively low voltage gradient designed into the system (the length of 4.6 cm was too long, being selected on the basis of minimum conductivity of the arc, with no margin for tolerance, on the long side, during fabrication). In other words, it corresponded to the minimum point of the ER vs. σ curve for the stable arc, whereas, the length was slightly too long, resulting in an unstable arc condition.

Another possible contributing factor in the "noise," restrike, imperfect current transfer problem noted may well have been an other than normal vacuum switch, damaged in previous tests by virtue of faulty switching procedure.

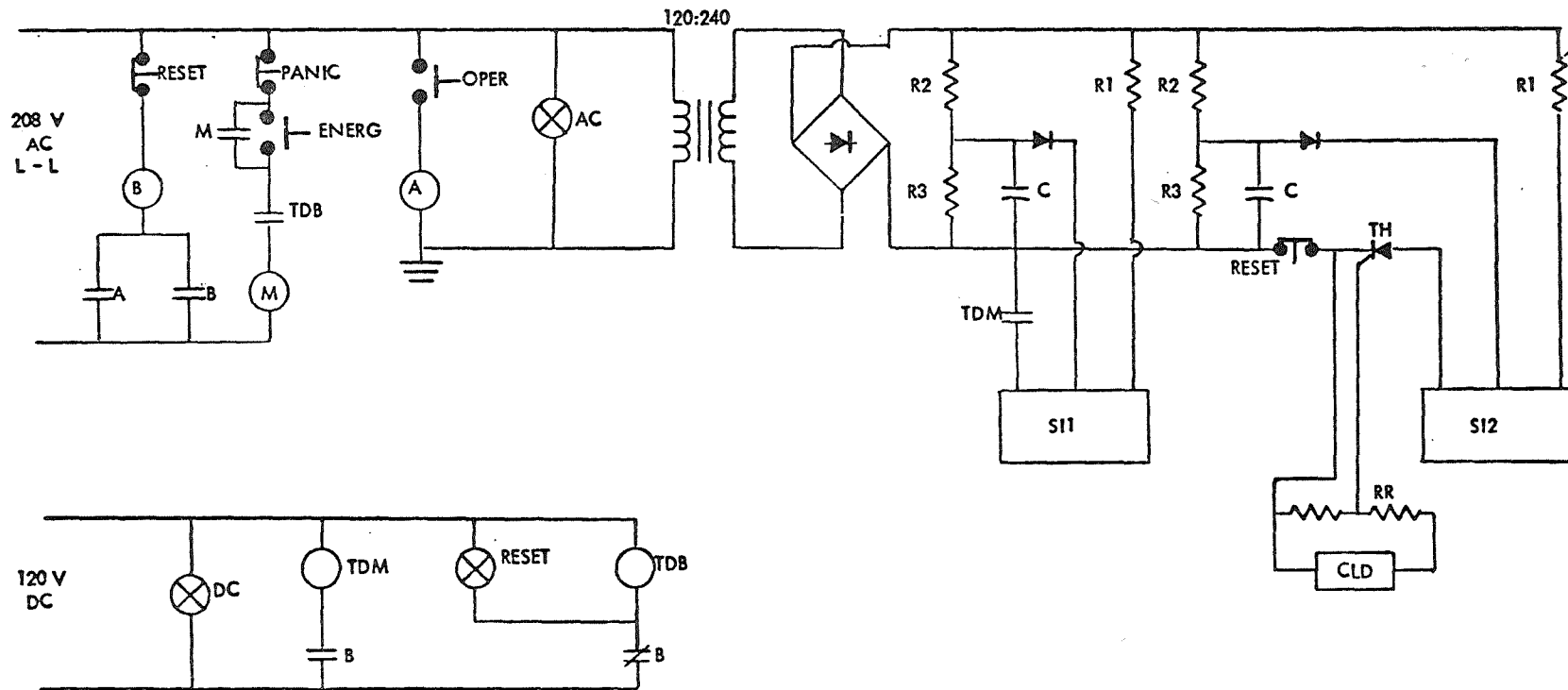


Figure 39 The Control Circuit

S11 = solenoid for the vacuum breaker I1
 S12 = solenoid for the vacuum breaker I2
 RR = voltage divider
 R1 = 1.5K Ω 10W
 R2 = 1.6K Ω 20W
 R3 = 500 Ω 5W
 C = electrolytic capacitor

The voltage of the rectifier side of the interrupter did not increase above 15% of the rated voltage, being effectively suppressed by the combination of the varistors and the capacitor. The voltage at the locomotive became negative for a very short period, contrary to the calculations and expectations. This effect was attributed to the fact that the track was rusted, and it introduced a relatively high resistance between the ground and the locomotive and thus in the FWD circuit.

The load current proved lower than anticipated (120-170A, instead of higher than 200A). This was the reason for the increase of the time to vaporize of the CLD. For safety the back up contactor was set to open very quickly; which it did; once before the CLD had changed state.

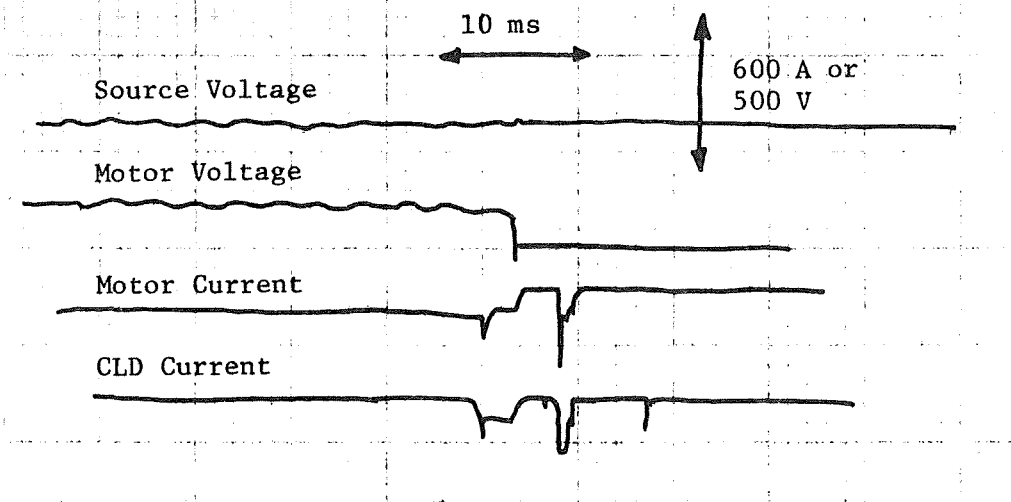


Figure 40. Field Test Results

5.2 The Short Circuit Tests

Because of its very short time to operate, the CLD is extremely useful for the limiting of short circuit currents. A high speed mechanical switch that would commutate the fault current to the CLD, as well as a suitable device that would sense the presence of the short circuit and trigger this commutating switch were not available at the time of the tests; therefore, the CLD was connected continuously and the fault applied to the circuit. No suppressing schemes were utilized in these tests because of possible adverse results that the presence of the suppressors would have on the short circuit current rate of rise.

The CLD and the Test Circuit

The CLD for the short circuit was similar to the one used in the normal load interruption test; the only difference being that it had four parallel bores instead of two, so that it had a larger current capacity.

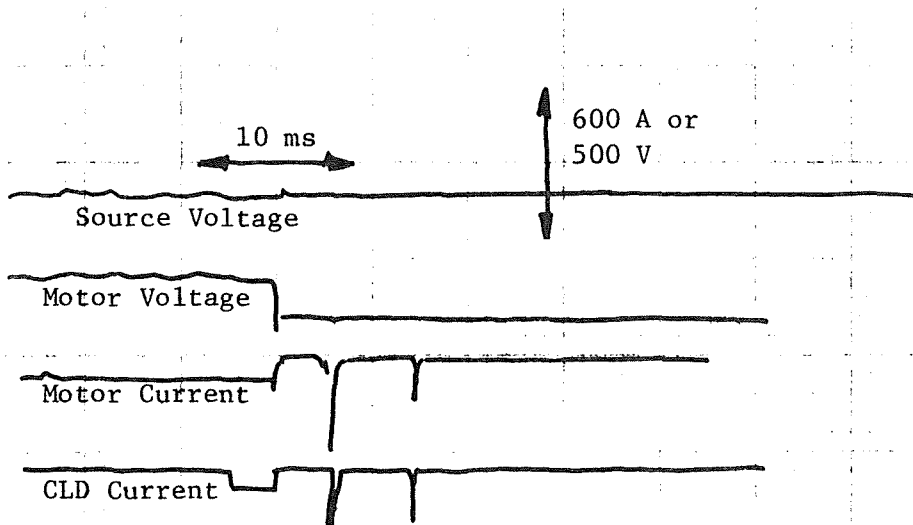


Figure 41. Field Test Results

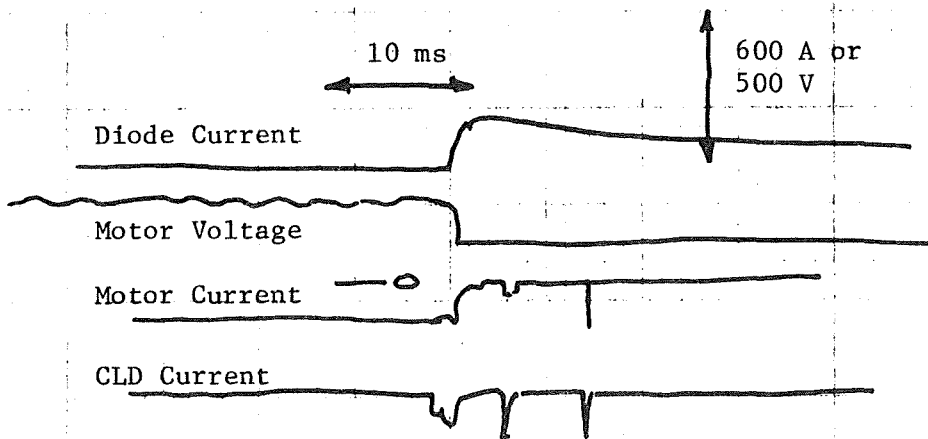


Figure 42. Field Test Results

The system impedance to the rectifier terminals was calculated as $z = 0.0228 + j 0.066$ ohms, from which system inductance is calculated as 0.175 henrys. Using the simplistic approach for calculating rate of rise of current discussed in Section 4.3, i.e., $di/dt = V/L$, the rate of rise was predicted to be 1.71×10^6 amperes/second. Calculating the time to vaporize using equation A-11 (discussed in the appendix) and with $I(0) = 0$ yields a time to vaporize of 0.00074 seconds, permitting the current to reach a value of $0.00074 \times 1.7 \times 10^6 = 1250$ amperes (predicted).

Because of the current values involved and the desire to use a commercially available 1250 ampere contactor, the CLD was hard wired into the circuit, using it as a fuse, and to impose a short circuit to the system through the conventional contactor.

A resistor, sized to pass a desired level of limited current, after CLD operation, was placed in parallel with the CLD, as shown in Figure 43.

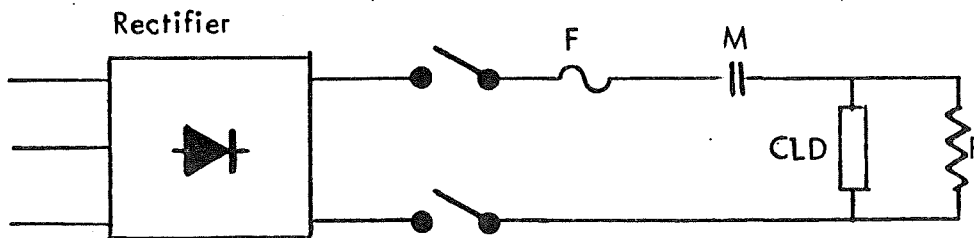


Figure 43 Test Circuit for the Current Limiting Short Circuit Field Test

M = 1250 A contactor
 R = low valued resistor
 F = 400 A fuse

Tests were run with values of R between 0.25Ω and 0.4Ω , thus permitting steady state short circuit fault currents in the range 750 to 1200A to flow after the CLD vaporized.

Test Results

Figure 44 depicts the rectifier current for the case of a parallel resistor of 0.25Ω . As calculated from the oscillogram, the rate of rise of the short circuit current was 2.03 KA/ms. This represents a circuit inductance of 0.153 mH. The steady state current was 1031A, which means that an additional resistance of 0.053Ω existed in the circuit, due to cables, shunt resistors and connections. The 0.7 ms time to vaporize permitted a peak current of $0.7 \times 2030 = 1421A$ at which time the paralleled resistor, R, permitted a 1031A current to flow.

Figure 45 also shows the current of the rectifier for the same paralleled value of 0.25Ω . The same value of steady current is obtained; however, the rate of rise of current of greater, yielding an apparent inductance of 0.109 mH. This discrepancy is attributed to the occurrence of the short circuit at different points on the voltage waveform.

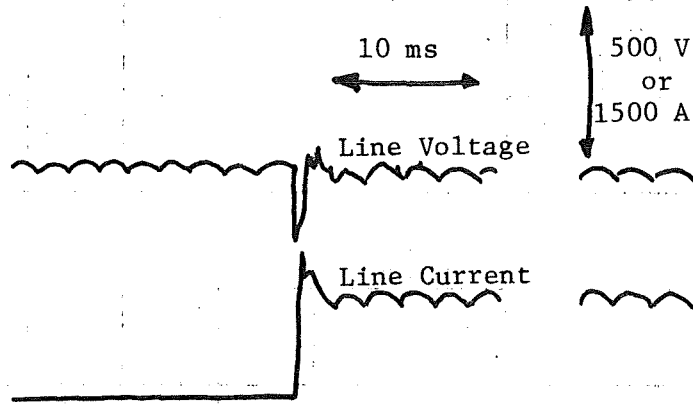


Figure 44. Short Circuit Test No. 1.
 Parallel Resistor: 0.25Ω
 Rate of Rise: 2.034×10^6 A/s
 Steady State Current: 1031 A

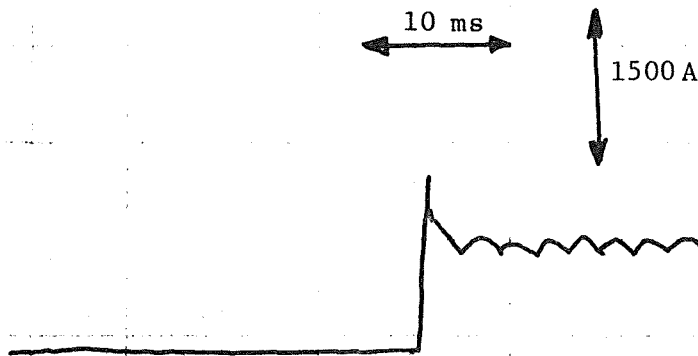


Figure 45. Short Circuit Test No. 2.
 Parallel Resistor: 0.25Ω
 Rate of Rise: 2.85×10^6 A/s
 Steady State Current: 1031 A

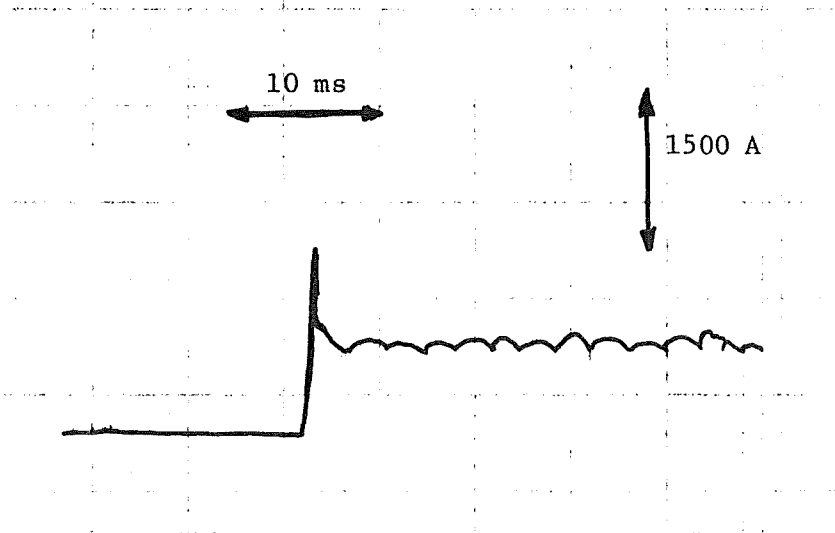


Figure 46. Short Circuit Test No. 4
 Parallel Resistor: 0.3Ω
 Rate of Rise: 2.4×10^6 A/s
 Steady State Current: 890 A

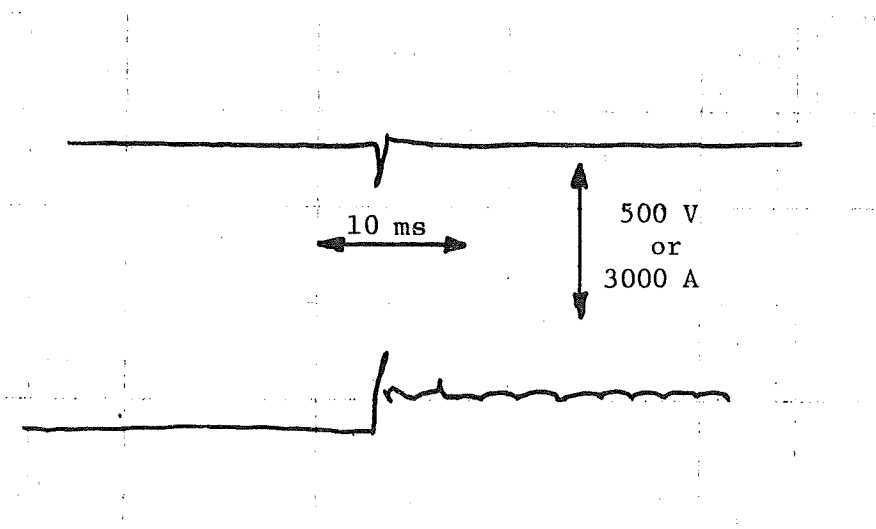


Figure 47. Short Circuit Test No. 6.
 Parallel Resistor: 0.4Ω
 Rate of Rise: 2.7×10^6 A/s
 Steady State Current: 703 A

Figure 46 and 47 show the short circuit fault of the supply for the cases of 0.3Ω and 0.4Ω parallel resistance, respectively. In Figure 49 the supply voltage is also recorded. It dips to about 55% of its normal value during the 0.6 ms of the duration of the short circuit, but it comes back as soon as the CLD performs its current limiting function.

6.0 CONCLUSIONS AND RECOMMENDATIONS

The basic objective of this study was to demonstrate that the CLD could be successfully used for high speed DC switching and current limiting in a full size system with motor loads. The anticipated voltage surges, with no suppression devices, did manifest themselves as predicted analytically. Tests on the laboratory system helped to obtain an understanding of the nature of the overvoltages and to develop the method of calculation for what to expect with surge suppression devices.

The overvoltage suppression techniques developed in the laboratory models were successfully applied in the field tests and no significant surges were encountered. A computer program was written to simulate the operation of the CLD and the surge suppressors. The results matched very well with the test results.

Because of the low (approximately 20-25V) arc voltage developed by the vacuum switches, care must be taken to insure a suitable margin of safety between the voltage of commutation existing across the CLD and the vacuum switch arc voltage. Also the design procedure of selecting CLD bore length for maximum conductivity, based on long bore length and low voltage gradient must be examined in view of the possible unstable arc and restrike if the bore length is too long.

The field tests indicate that the CLD can be a very effective device for limiting the short circuit current level when used as a device injected in series with the fault and when paralleled with a resistor sized to permit a desired level of sustained fault current (prior to fuse clearing).

Since the probable rate of rise of short circuit current is around $2-3 \times 10^6$ A/s and the time available for peak limiting is much less than the circuit time constants, this is a nearly linear rate of rise and the time for the CLD injection and vaporization can be easily estimated. However, a very rapid opening switch with high arc voltage will be required for implementation. Either an Exploding Bridge Detonator switch as described in Section 4.2 or a spring loaded switch with (1) small mass, (2) low inductance trip coil, and (3) relatively large gap length would suffice for this application. Since it is commutating the current into the low resistance CLD, interrupting capability for this switch is not a consideration.

In addition, a fault sensor, capable of detection and decision in the microsecond time frame, must also be used to actuate the switch. Such a sensor would have to make its decision on a combination of variables; such as current level and rate of rise, in order to detect at a relatively low current level and still not to be subject to false tripping under momentary overloads due to motor starts, etc. This requirement was discussed in Section 4.1.

Recommendations and suggestions for future work include the following:

1. elimination of the need for machined cylinders and pistons necessary for pressurizing/reset;
2. incorporation of high resistance wire, integral to the CLD for fault current limiting;
3. addition work in the materials and sealing areas to decrease possible mercury penetration into the casting material;
4. testing of the CLD, in the field, with a decoupled CLD/Interrupter switching circuit.

1. Elimination of Need for Machined Cylinders and Pistons

The units designed and tested to date under the USBM contracts have utilized either bellows or machined precision cylinder and piston arrangements to achieve pressurization and reset action (i.e., forcing liquid mercury back into the bores) after CLD operation.

A possible scheme for accomplishing this is to use either Buna or Neoprene rubber type washers (similar to bottle stoppers) immersed in the liquid mercury. The washer would be impervious to mercury but would have resiliency to provide additional volume to accommodate mercury forced out of the bores when the CLD operates. In addition a valve and filling provision for filling and sealing the CLD assembly under pressure would be necessary. This configuration should result in a less costly CLD.

2. Incorporation of Integral Resistance

In fault current limiting, it is desirable to "pinch off" the rising fault current and to then restrain it to a predetermined level by having a by-pass resistor in parallel with the CLD. In the interest of a smaller volume assembly and economy, it should be possible to use a high resistance conductor, such as Nichrome type alloys, incorporated and connected from end cap to end cap; thus providing the desired by pass resistor.

3. Materials and Sealing

In the units build and tested under the USBM contract, Sauereisen cements have been used as the casting material to contain the alumina bores within the insulating housing.

Mercury is compatible with Sauereisen and no troubles were experienced in this respect.

However, if a more active metallic filler for the CLD, such as sodium, potassium or NaK were to be used, the water based Saurereisen cements probably will not be compatible and a program for determining suitable casting materials compatible with these metals should be commenced. Appendix C presents a discussion of the casting materials and sealing technique used in this work.

4. Testing a Decoupled CLD/Interrupter Switching Circuit

For a field installation of a CLD switching scheme, isolation between the voltage drop sensed across the CLD and the control circuitry power supply

must be achieved because of the lack of a common ground. APPENDIX D details a proposed circuit for achieving this objective. This circuitry was tested in the laboratory and functions satisfactorily but it has not been field tested.

APPENDIX A - Design Equations and Procedures

The derivation of the design relationships for a change of state CLD was presented in the previous USBM report⁽⁵⁾. Only the derived equations will be presented here.

In designing a CLD for a specific application, the length and radius of the bore tubes used must be determined, as well as the number of parallel bores necessary. These relationships are established based on the circuit voltage, the current prior to change of state, the arc voltage developed by the switch which inserts the CLD into the circuit and the arc power per unit of wall area to which the bore is subjected.

Several guidelines have been determined by experience gained in the design and test of CLD units. They are:

1. Mercury is an ideal liquid metal for use in CLD because of its liquidity at and over the normal operating temperature range. However, if the "cold" resistance of the device is a critical feature - either because of the high level of current through the device at the time of insertion or because of limited arc voltage developed by the insertion switch, it may be necessary to use a material with lower resistivity such as NaK, K, or Na. Because of handling and CLD loading problems associated with these corrosive materials, mercury is preferred.
2. A pressure of 3.0 atmospheres on the mercury is sufficient to insure CLD reset action after the circuit is interrupted.
3. A voltage gradient of 100 volts/centimeter should probably be used to insure a stable arc characteristic, even though (theoretically) the stable arc can be achieved at other, lower values, based on a combination of voltage gradient and bore radius. (Refer to Figure A-1, derived in Reference 1.)
4. If possible, bore radius, should be selected to keep the arc power per unit of wall area down around 5000-10000 watts/cm². This may not be possible without utilizing an excessive, non-feasible number of very small radius bore tubes. Certainly, the lower this value, the longer life expectancy of the CLD.
5. The relationship between $i(t)$, time to vaporize, bore radius, R, and number of parallel bores, q, given by⁽⁵⁾

$$\int_0^t i(t)^2 dt = q^2 R^4 K \quad (A-1)$$

based on the conservation of energy balance, yields acceptable accuracy for performance calculations. For Hg, at 3 atmospheres, $K = 61.63 \times 10^6$. K for other materials and pressures is presented in Reference 1.

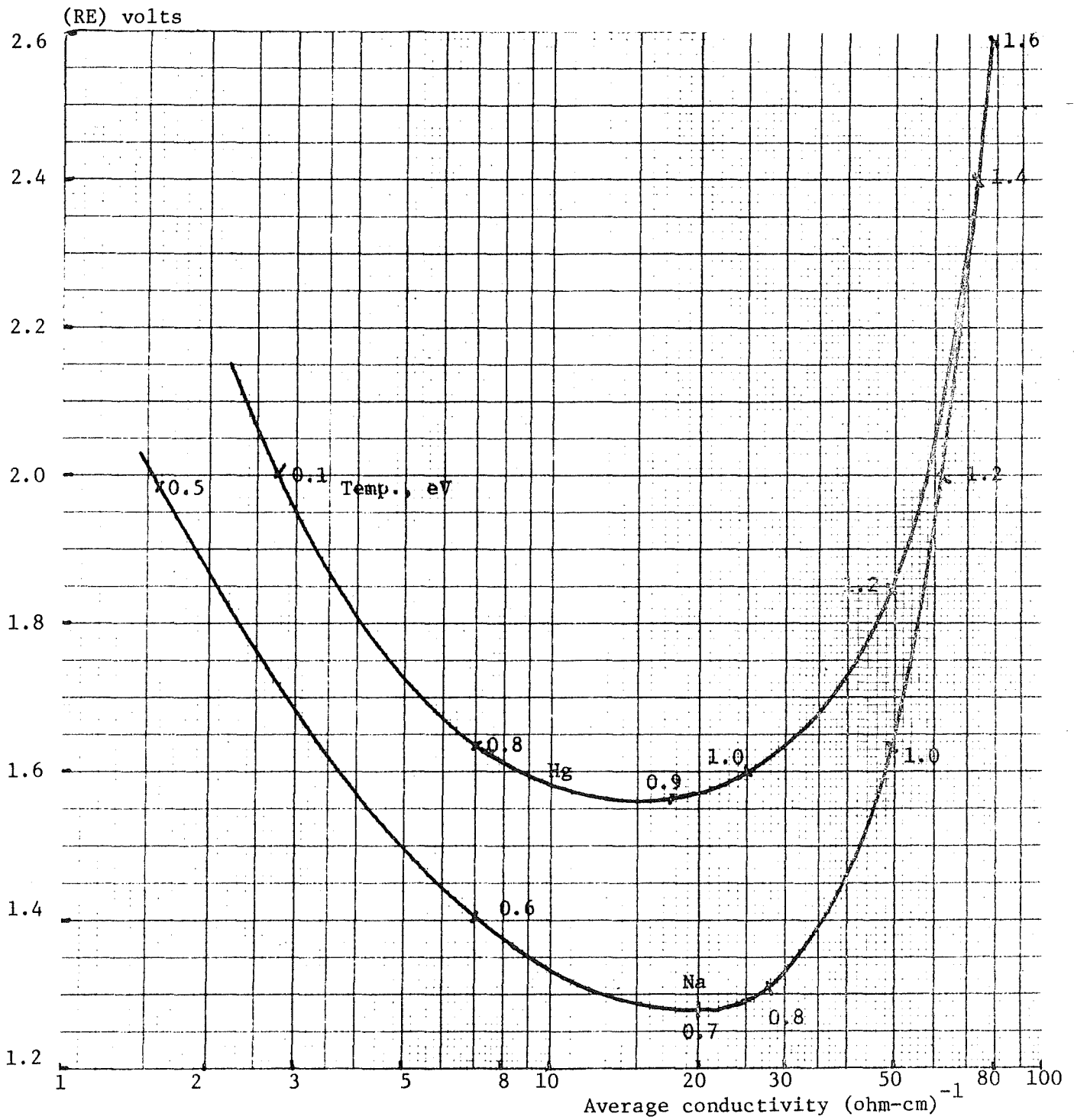


Figure A-1. (RE) vs. σ_{ave} , Characteristic for Hg and Na Vapor Arcs at 3 Atmosphere Pressure.

Design for Switching a Constant Current

Assume it is desired to design a CLD for switching a current, I , in a circuit with voltage V and vaporization (change of state) is to occur in t seconds, where:

$I = 1500$ amperes, $V = 300$ volts, $t = 0.0005$ seconds. The length ℓ , required is:

$$\frac{V}{\ell} = 100 \text{ or } \ell = \frac{300}{100} = 3 \text{ cm} \quad (\text{A-2})$$

From (A-1)

$$q^2 R^4 = \frac{I^2 t}{K} \quad (\text{A-3})$$

or

$$q^2 R^4 = \frac{1500^2 \times 0.0005}{61.63 \times 10^6} \quad (\text{A-4})$$

As a first trial, assume that $q = 5$ is an acceptable number of parallel bores. From (A-4), with $q = 5$, $R = 0.292$ cm.

Selecting R from the sizes of alumina bore tubes commercially available yields, $R = 0.03$. Using $R = 0.03$, $q = 5$ in (A-3) yields a time to vaporize of $t = 0.00055$ seconds.

The value of: $E \times R = V/\ell \times R = 300/3 \times 3/100 = 3$ is checked for conductivity after change of state, using Figure A-1, and is estimated at $100 \text{ (ohm-cm)}^{-1}$. The arc power per unit of wall area is calculated from (5)

$$\frac{P}{A} = \frac{E^2 R \sigma}{2} = \frac{100^2 \times 0.03 \times 100}{2} = 15000 \text{ watts/cm}^2 \quad (\text{A-5})$$

The "cold" resistance of the CLD is calculated as:

$$\Omega_o = \frac{\rho \ell}{\pi R^2 q} = \frac{96}{10^6} \times \frac{3}{\pi \times 0.03^2 \times 5} = \frac{2.037}{10^2} \text{ ohms} \quad (\text{A-6})$$

The switch used for insertion must develop a minimum arc voltage of

$$V_{\text{arc}} = \Omega_c I = \frac{2.037}{100} \times 1500 = 30.56 \text{ volts} \quad (\text{A-7})$$

The resistance after vaporization is:

$$\Omega_v = \frac{\ell}{\sigma \pi R^2 q} = \frac{3}{100 \times \pi \times 0.03^2 \times 5} = 2.122 \text{ ohms} \quad (\text{A-8})$$

yielding a current, after vaporization, which must be interrupted of:

$$I_i = \frac{V}{\Omega_v} = \frac{300}{2.122} = 141.4 \text{ amperes} \quad (\text{A-9})$$

If any of the above are not satisfactory another value of q must be chosen and the calculations repeated. For example, if $q = 6$ is chosen,

$R = 0.027$; use $R = 0.025$ cm and:

$$\begin{aligned} t &= 0.0003 \text{ seconds} \\ E \times R &= 2.5 \\ \sigma &= 75 \text{ (ohm-cm)}^{-1} \\ \frac{P}{A} &= 9375 \text{ watts/cm}^2 \\ \Omega_c &= 0.0244 \text{ ohms} \\ V_{\text{arc}} &= 36.67 \text{ volts} \\ \Omega_v &= 3.395 \text{ ohms} \\ I_i &= 88.37 \text{ amperes} \end{aligned}$$

If still not satisfactory, it may be necessary to decrease the voltage gradient and assume the probability of arc restriking, or manipulate the various variables in such a manner as to achieve the required performance.

Design for Switching A Rising DC Short Circuit Current

The design procedure for this application is similar to the previous example, except the current is given by:

$$i(t) = I(0) + \left(\frac{\Delta I}{\Delta t}\right) t \quad (\text{A-10})$$

where $I(0)$ is the current at $t = 0$ and I/t is the rate of rise of current. The relationship given in (A-1) becomes:

$$I(0)^2 t + I(0) \left(\frac{\Delta I}{\Delta t}\right) t^2 + \left(\frac{\Delta I}{\Delta t}\right)^2 \frac{t^3}{3} = q^2 R^4 K \quad (\text{A-11})$$

Determination of t is based on how high an amplitude of $i(t)$ can be tolerated before the CLD vaporizes and changes state. If t_s is the total time to decide to switch, plus the switching time, the current will have reached a value of I_s , where:

$$I_s = I(0) + \left(\frac{\Delta I}{\Delta t}\right) t_s \quad (\text{A-12})$$

and the required arc voltage for switching will be:

$$V_{\text{arc}} = I_s \Omega_c \quad (\text{A-13})$$

The design procedure (otherwise) proceeds as in the previous example.

Design for Switching A Rising AC Short Circuit Current

Note that $i(t)$ can be either symmetrical or, as an extreme, fully offset and represented by:

$$i(t) = \sqrt{2} I \sin \omega t \quad \text{or} \quad i(t) = \sqrt{2} I (1 - \cos \omega t) \quad (\text{A-14})$$

where I is the rms value of fault current from which, two expressions relating the variables are obtained as:

For the symmetrical case:

$$\frac{t}{2} - \frac{\sin 2\omega t}{4\omega} = \frac{30.81 R^4 q^2 \times 10^6}{I^2} \quad (\text{A-15})$$

For the full offset case:

$$\frac{3t}{2} - \frac{2}{\omega} \sin \omega t + \frac{1}{4\omega} \sin 2\omega t = \frac{30.81 R^4 q^2 \times 10^6}{I^2} \quad (\text{A-16})$$

These equations can be solved either by iterative techniques or graphically. The graphical approach is preferred since it enables visualization of new choices of R and q in the design process. Both the right and left hand sides of the above equations plot as straight lines on log-log paper. Such a plot of the equations is shown in Figure A-2. \bar{X} and \bar{Y} are the plots for the left hand side of equations (A-15) and (A-16) as a function of time. The other line is the right hand side of the equations for chosen values of R and q , denote d as \bar{Z} , as a function of current. The particular \bar{Z} vs. I shown in Figure A-2 is for $R = 0.05$ and $q = 3$. To obtain the time of vaporization for an rms current of 3000 amperes, for example, enter Figure 2 from the horizontal axis at a value of 3000 amperes. Go vertically to an intersection with the \bar{Z} line. For a solution to (A-15) or (A-16), $\bar{Z} = \bar{X}$ or \bar{Y} . Thus go horizontally until intersection with \bar{X} and \bar{Y} curves, then drop vertically to determine the times of 0.00013 (for full offset) and 0.0004 (for symmetrical wave) seconds. From this, we know that the actual time of vaporization for a 3000 ampere rms wave will lie between these two time limits, depending on the degree of asymmetry present. This solution assumes a negligible value of current level prior to CLD insertion (in effect, a very high speed switch used for insertion).

The above examples demonstrate the design procedures to follow for specific applications.

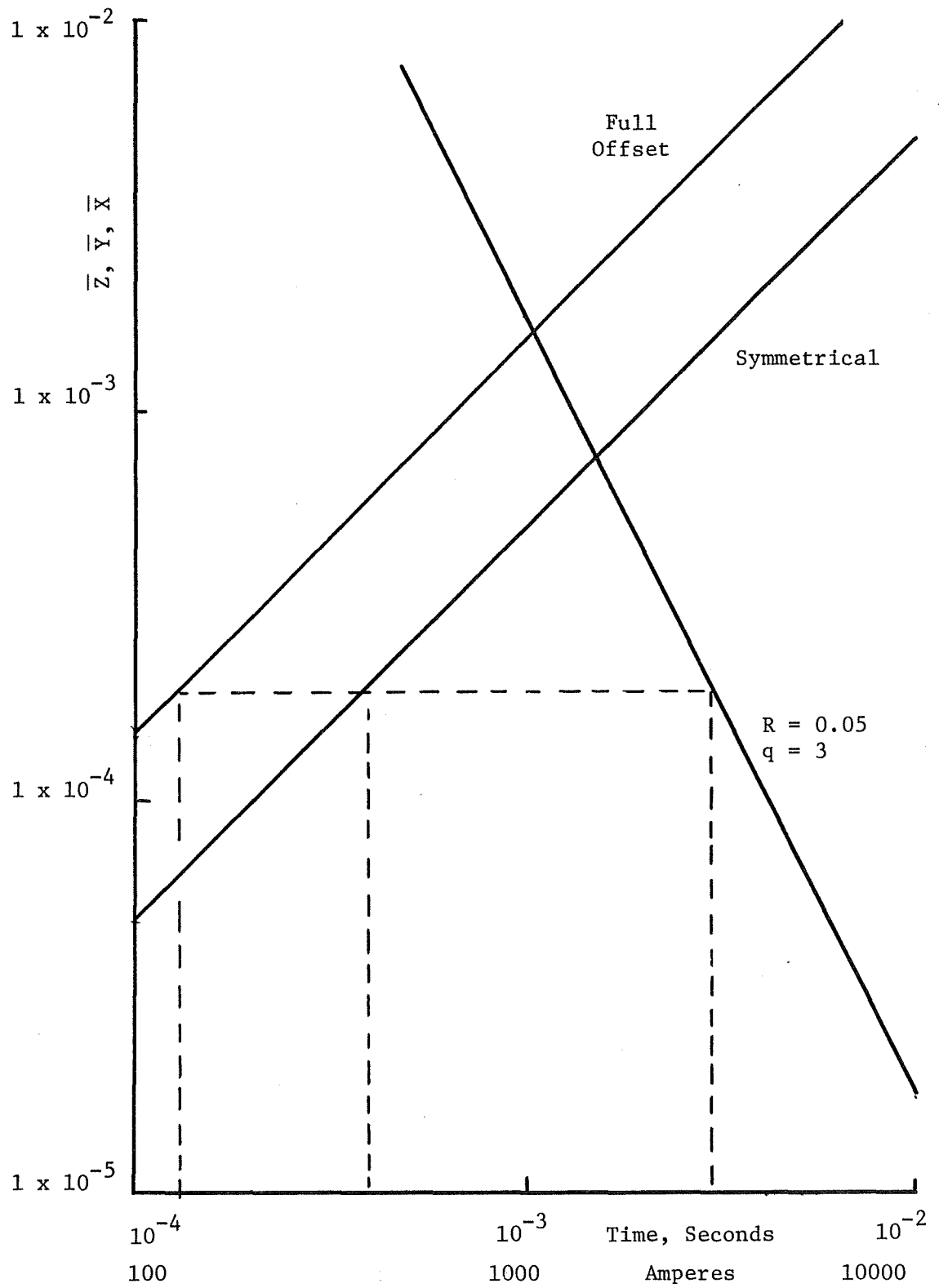
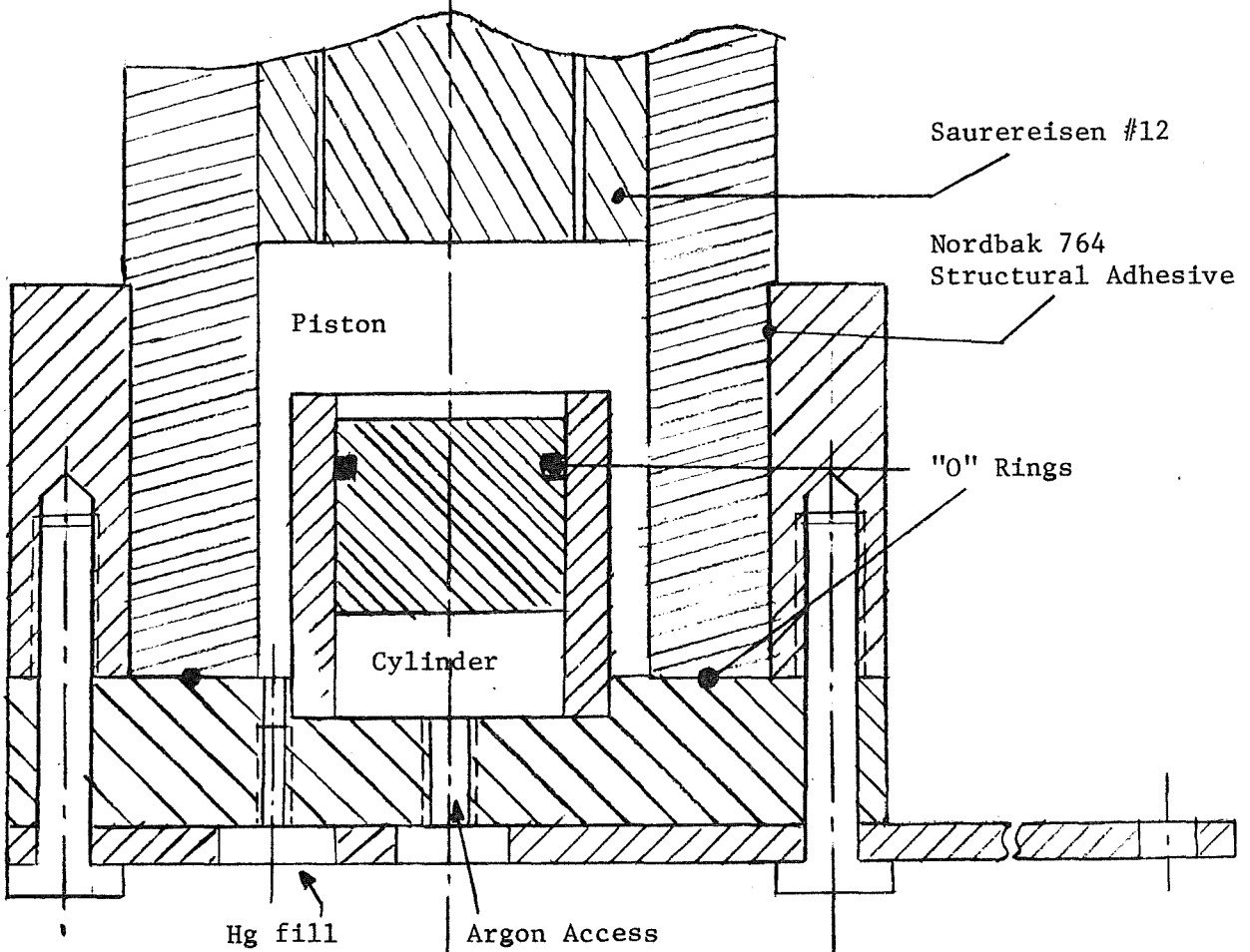
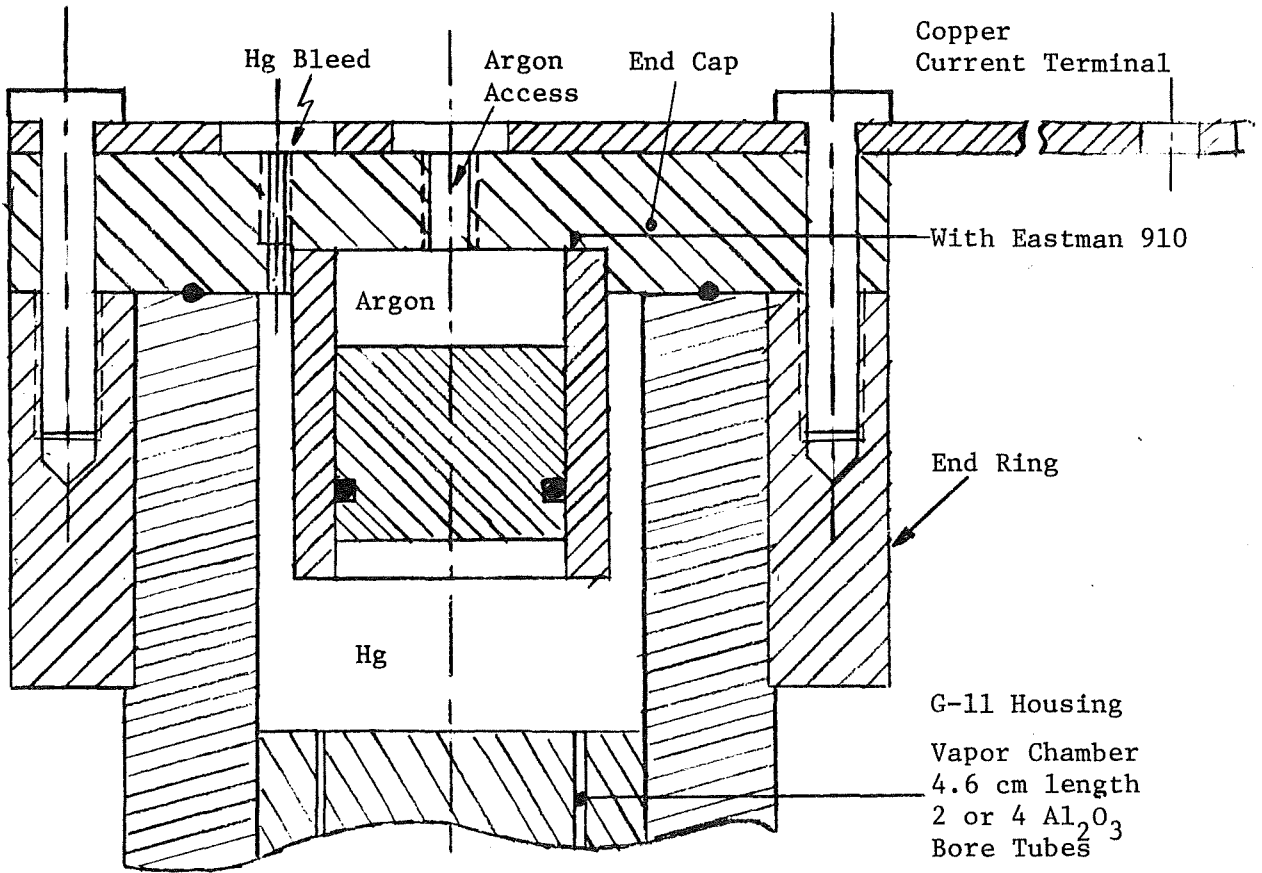
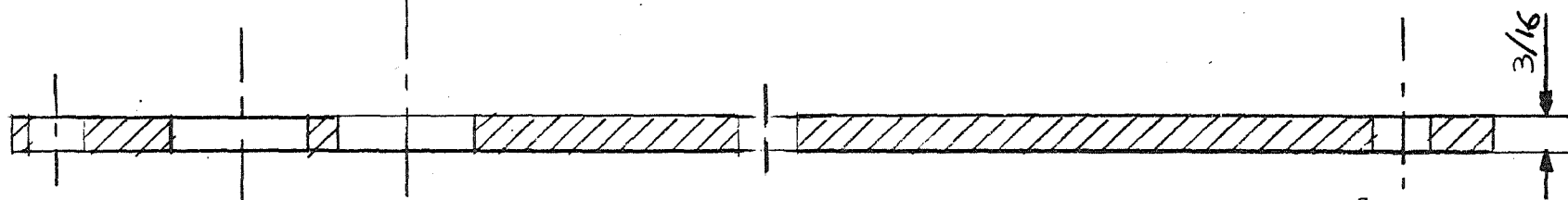
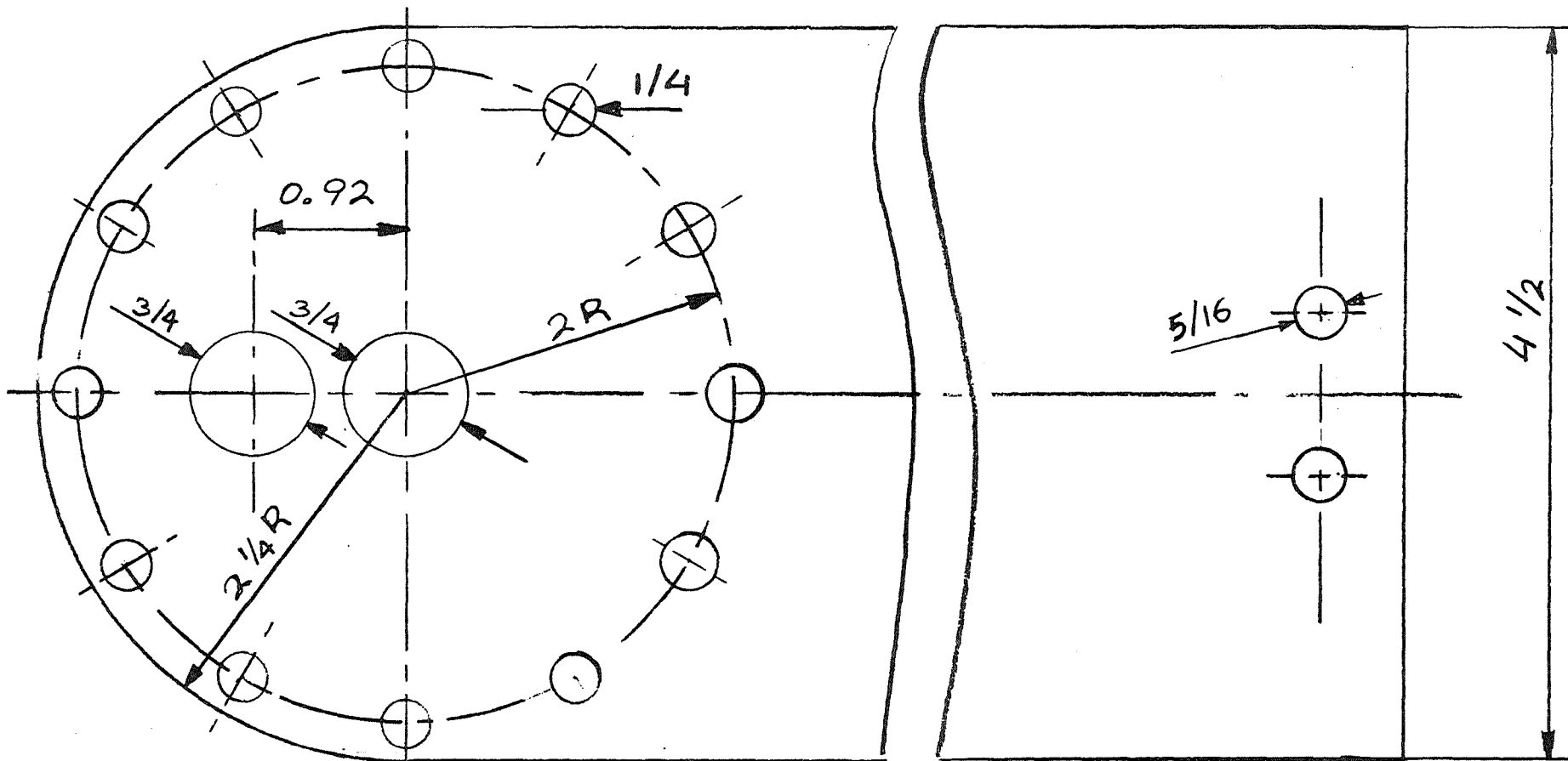


Figure A-2

APPENDIX B
Detail Drawings of CLD

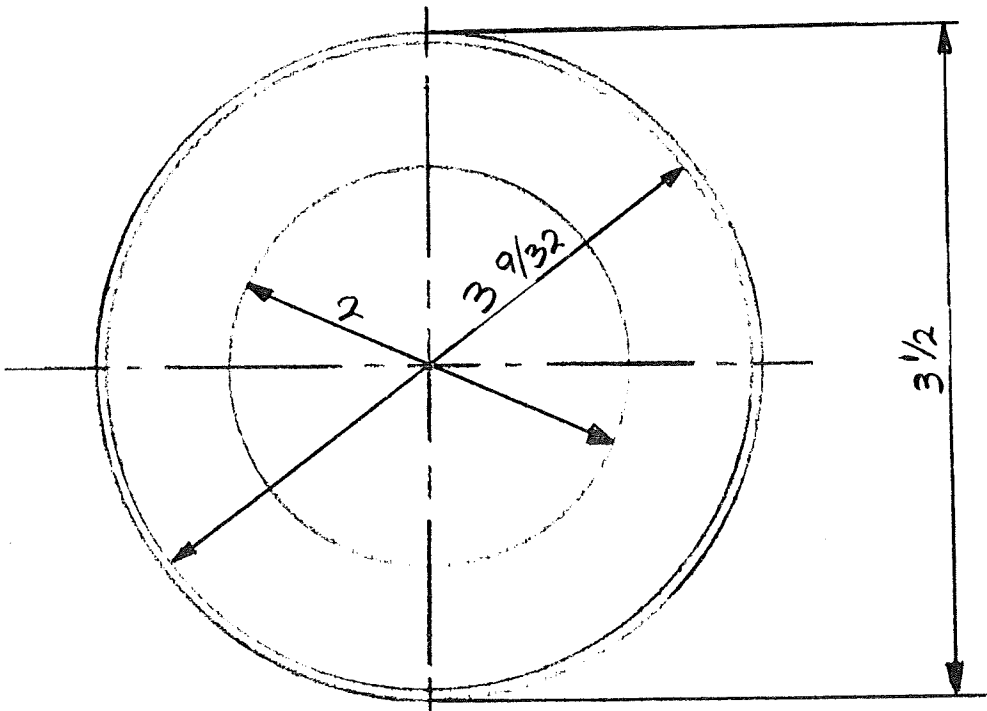
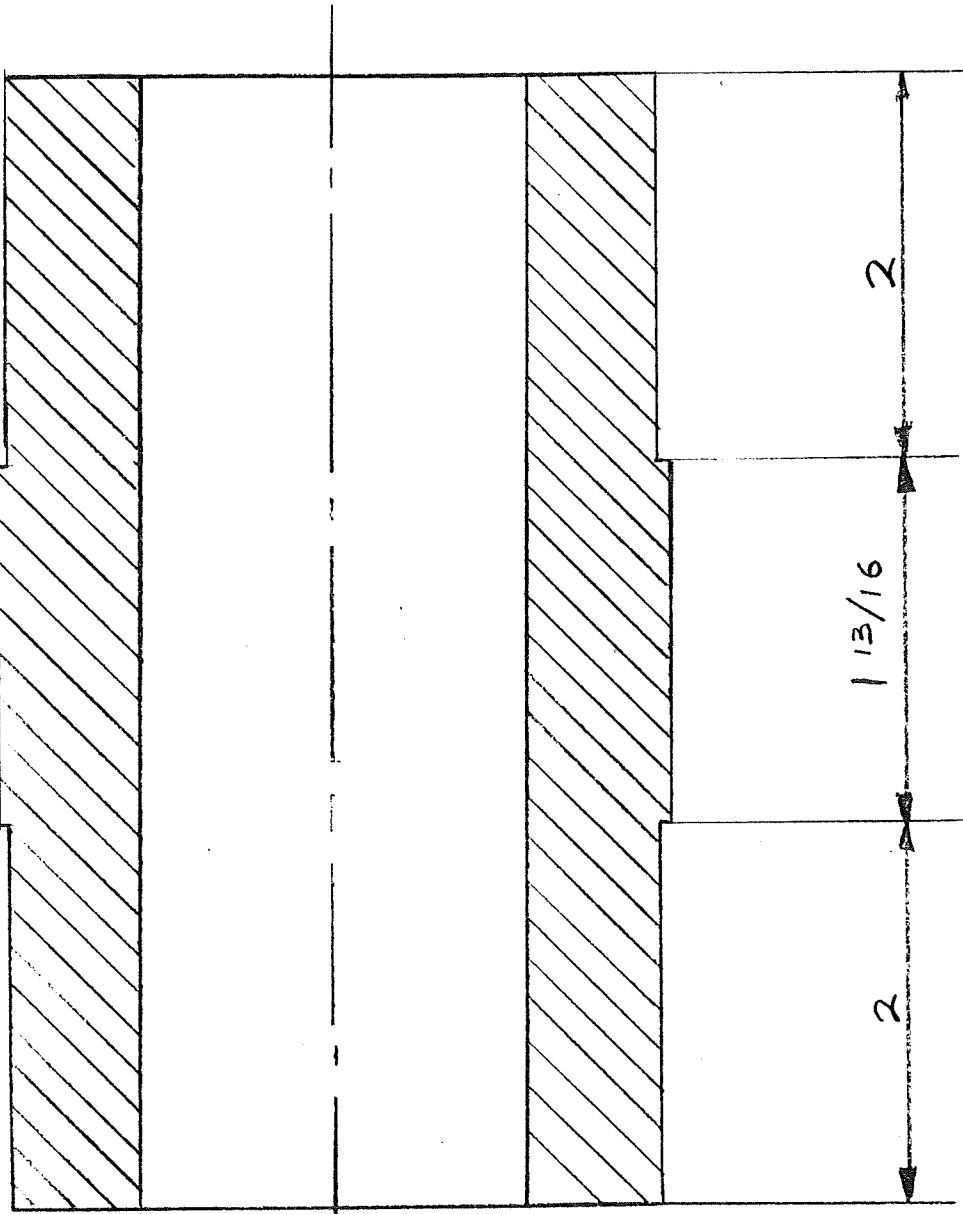


Assembly



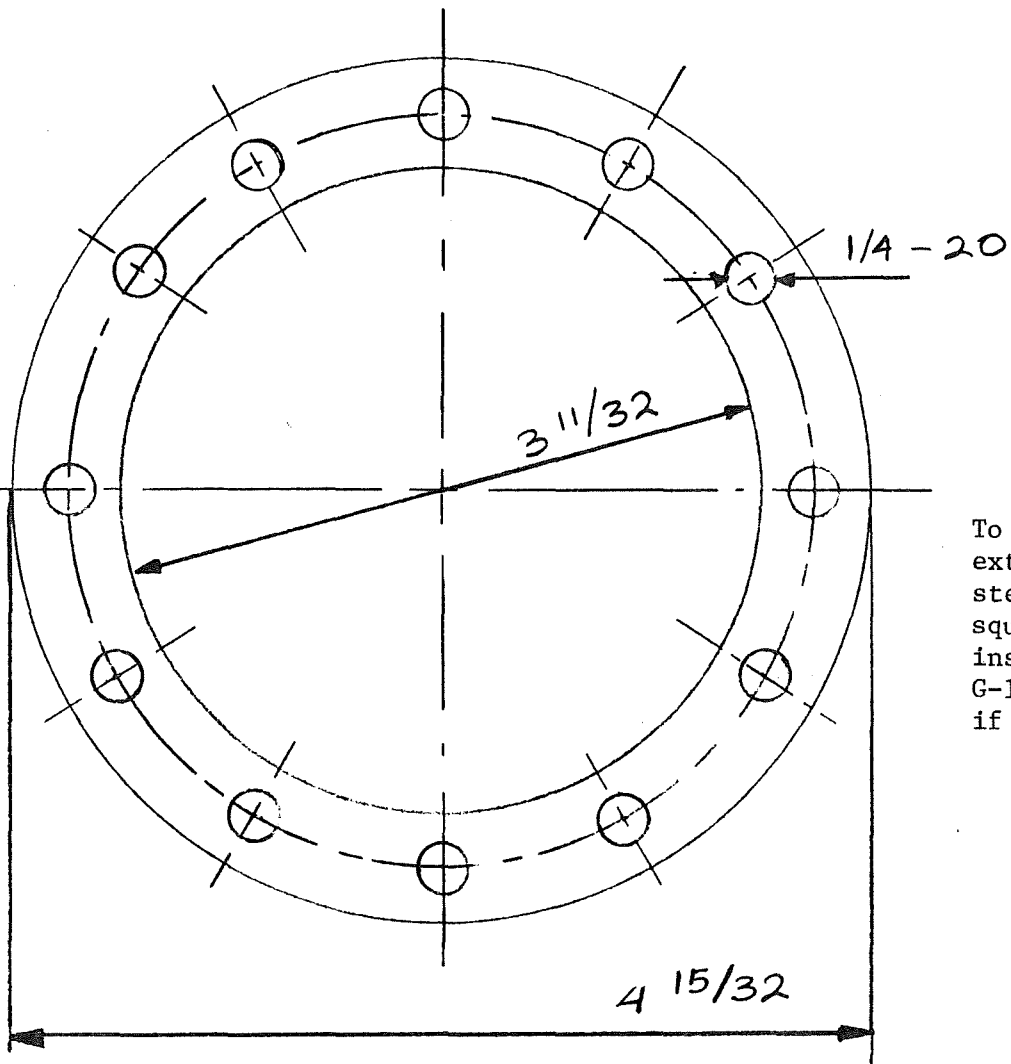
Current Terminals, 2 Required

Copper

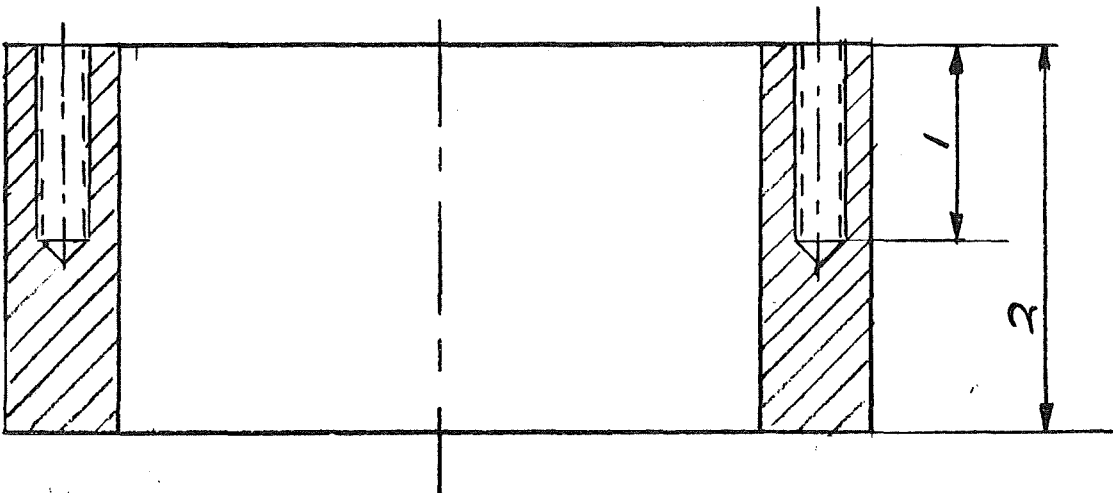


1 required G-11

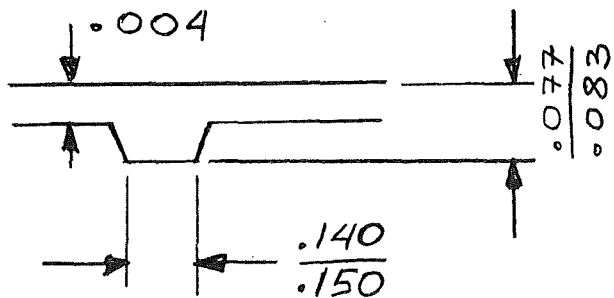
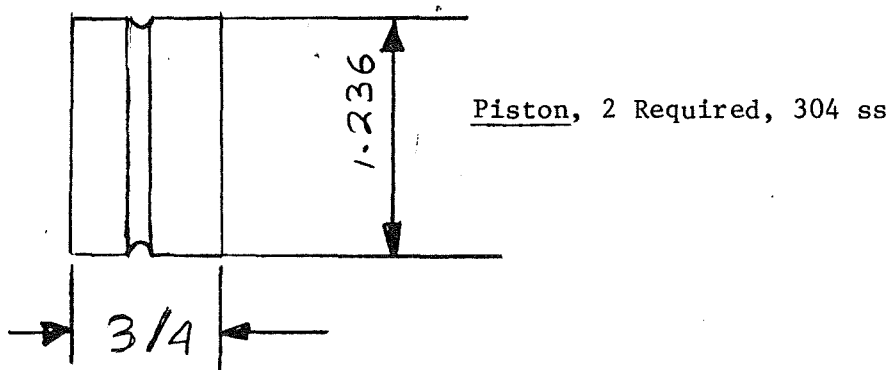
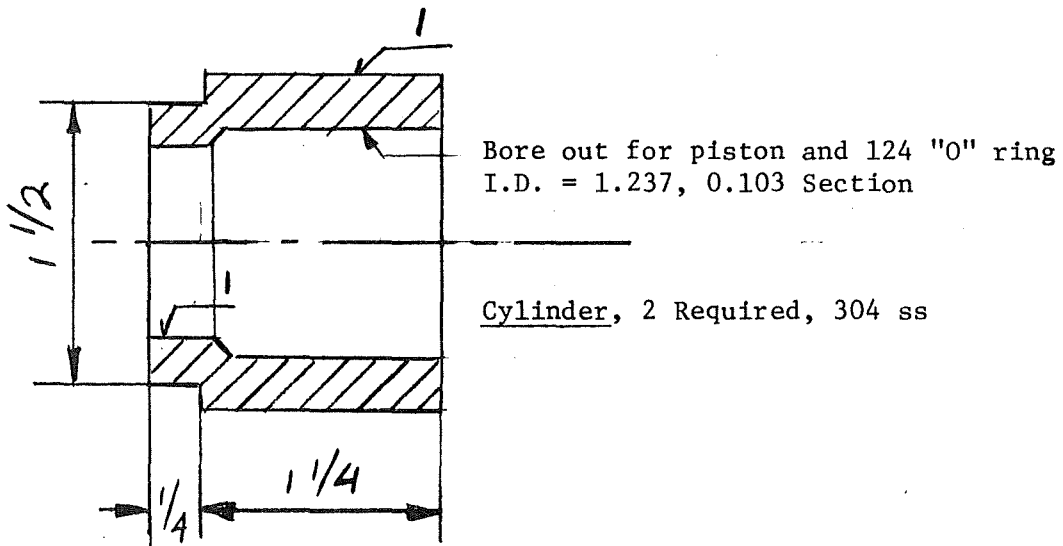
Insulated Housing



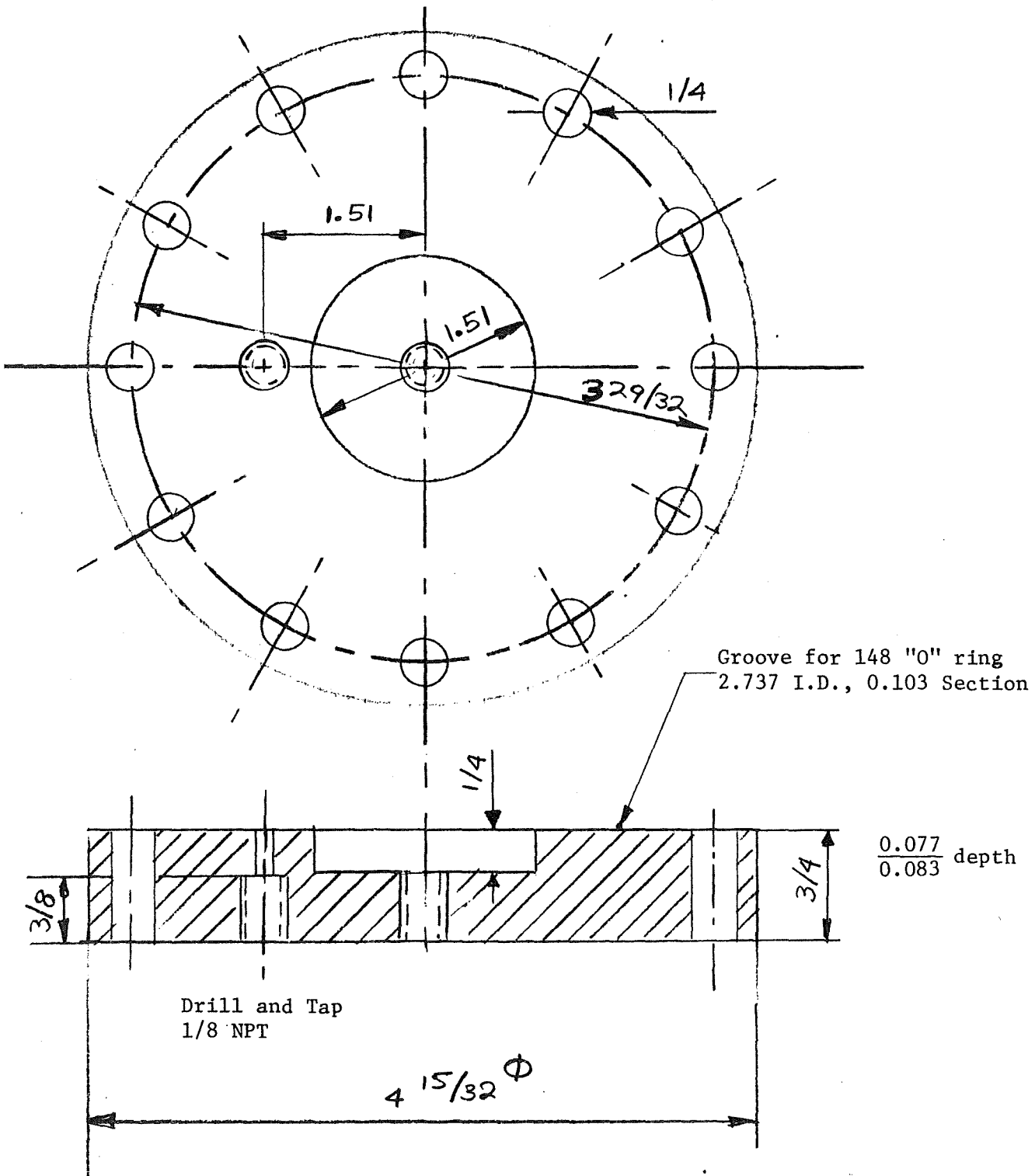
To be made from double extra heavy seamless steel pipe, nominal 4", square off ends, bore inside to true neck down G-11 housing for clearance, if necessary.



End Ring, 2 Required



"O" Ring Groove Detail



End Caps, 2 Required, 303 ss

APPENDIX C

Notes on Casting Material,
Structural Adhesive and Sealing Used

In earlier CLD units, various Saurereisen casting materials were utilized and the results of various tests were that Saurereisen #8 was the most satisfactory. However, even the slight shrinkage encountered was objectionable because it necessitated thorough (and often unseccessful) sealing procedures to prevent mercury migration between the Saurereisen casting and the inner wall of the insulating tubing. During the course of this program, Saurereisen provided a new material, originally designated as #8X and later as #12, which included Iron Chromite to control shrinkage and to be mixed with Monoaluminum Phosphate rather than with water.

This material exhibits (apparently) zero shrinkage if not exposed to elevated (above 100°C) temperatures for prolonged periods. The castings (successful) were cured at room temperature over a period of a few days (4 days appears sufficient). In one of the units, the alumina was cast in the insulating housing, then the end rings (see Appendix B) were emplaced with structural adhesive and the assembly cured at 150°C for 2 hours. The Saurereisen did shrink excessively so units fabricated after that experience were in the sequence of installing end rings, cure, and then casting the bore tubes. The Saurereisen powder was mixed with the monoaluminum phosphate in a proportion to yield a castable mixture.

A potentially useful casting material was located too late for evaluation but it does appear to have desirable properties and should be evaluated in future work. It is Calcium Alumina Cement, Aluminum Company of America (ALCOA Chemicals) CA-25C.

The structural adhesive used was Nordbak 764, obtainable from Rexnord, 4300 N. 127th Street, Brookville, WI, 53005, (414) 781-5204. In laboratory tests, shear strengths of 3000 pounds/square inch, with an adhesive layer 1/32 inch thick, were obtained.

The sealing technique used was to paint at least two coats of Epoxyn Enamel Series R, obtainable from Co-Polymer Chemicals, Inc., 12350 Merriman Road, Livonia, MI, 48150, over the surface of the Saurereisen and on the interface with and up the wall of the G-11 tubing.

Each coat of the sealant was allowed to room temperature cure for 24 hours.

The combinations used above did give satisfactory performance in the tests run but exhaustive life tests to insure the most desirable material selection should be conducted.

APPENDIX D

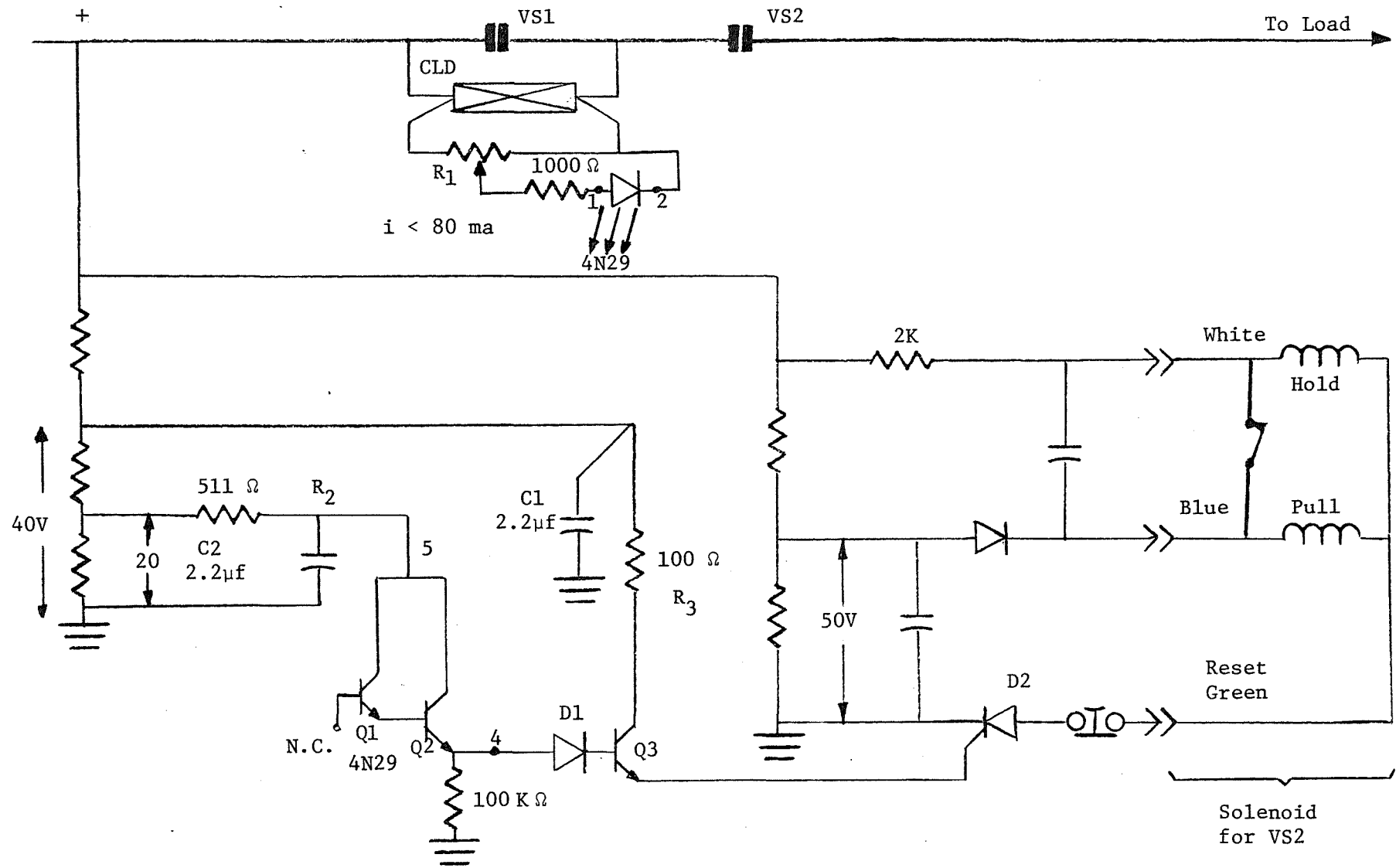
Decoupled CLD/Interruptor Switching Circuit

For a field installation of a CLD switching scheme, isolation between the voltage drop sensed across the CLD and the control circuitry power supply must be achieved -- otherwise the absence of a common ground presents problems (refer to Appendix C, USBM Contract Report #HO 357079 for a discussion of the problem). To circumvent the need for an isolated power supply (such as transformer isolation from an A.C. source, then rectified), an optically isolated circuit, powered from the DC circuit has been developed.

The optical isolation circuit is shown in Figure D-1. The 4N29 contains a gallium Arsenide infrared emitting diode optically coupled to a silicon photo Darlington transistor designed for 2.5 Kv isolation insulation level. Q3 is a high speed, medium power switching transistor, type 2N2219 which provides the gate trigger for an 2N690 thyristor. This thyristor is rated 25 amperes, 600 VFB and 150 ampere surge capability and can handle a very large vacuum switch or contactor solenoid.

Capacitors C1 and C2 provide power supply decoupling. The circuit operates as follows:

When vacuum switch VS1 opens and commutates load current into the CLD, the CLD vaporizes, changes resistance and nearly full line voltage appears across the voltage divider array, R1. Values are chosen to insure that 50-75 volts appear across CR1 (limited to 80 milli amperes through the 1,000 ohm resistor). CR1, when conducting, optically turns on the Darlington pair of transistors, Q1 and Q2. The current that turns on Q3 flows through R2. Current for the thyristor gate signal is derived through R3 (25 milli amperes at 3 volts, minimum). When thyristor 2N690 conducts, the solenoid is actuated, opening vacuum switch VS2.



- C1, C2 2.2 f
- Q1, Q2 } Motorola 4N29 (LED)
- CR1 } Motorola 4N29 (LED)
- Q3 T.I. 2N2219
- D1 1N969 Diode
- D2 2N690 Thyristor

Figure D-1

BIBLIOGRAPHY

1. T.J. Ramos, "Analysis and Design of Interrupting and Line Sectionalizing Schemes for Heavy Current DC Circuits Using Current Limiting Devices," (Unpublished Ph.D. Dissertation, School of Engineering, University of Pittsburgh, 1975).
2. Tseng-Wu Liao and Thomas H. Lee, "Surge Suppressors for the Protection of Solid State Devices," IEEE Transactions on Industry and General Applications, Vol. IGA-2, No. 1, Jan.-Feb., 1966.
3. General Electric Co., "Transient Voltage Suppression Manual," New York, 1976.
4. N.L. Industries, "Application Data. Varistors. General Characteristics."
5. H.B. Hamilton and T.J. Ramos, "Feasibility Study of the use of Current Limiting Devices in Interrupting and Sectionalizing of DC Circuits in Mines," Final Report, Contract #HO 357079, U.S. Bureau of Mines, Bruceton, PA.